

2RC MODEL BASED STATE OF CHARGE ESTIMATION OF LITHIUM-ION BATTERY

This thesis is submitted in partial fulfilment of the requirements for
the degree of

MASTER IN CONTROL SYSTEM ENGINEERING

Submitted by

ALI HOSSAIN MONDAL

Class Roll Number: -002110804006

Examination Roll Number: - M4CTL23002

Registration Number: -160198 of 2021-2022

Under the Guidance of

Prof. Ranjit Kumar Barai

Submitted to

Department of Electrical Engineering
Faculty of Engineering and Technology
JADAVPUR UNIVERSITY
KOLKATA-700032

November, 2023

Faculty of Engineering and Technology

JADAVPUR UNIVERSITY

Kolkata-700032

Certificate of Recommendation

This is to certify that Mr. Ali Hossain Mondal (002110804006) has completed his thesis titled, “**2RC MODEL BASED STATE OF CHARGE ESTIMATION OF LITHIUM-ION BATTERY**”, under the direct supervision and guidance of Prof Ranjit Kumar Barai, Department of Electrical Engineering, Jadavpur University. We are satisfied with his work, which is being presented for the partial fulfillment of the degree of Master in Control System Engineering of Jadavpur University, Kolkata-700032.

.....
Prof. Ranjit Kumar Barai

Dept. of Electrical Engineering
Jadavpur University, Kolkata-700032

.....
Prof. Biswanath Roy

Head of the Department
Electrical Engineering Department
Jadavpur University
Kolkata-700032

.....
Prof. Saswati Mazumdar

Dean
Electrical Engineering Department
Jadavpur University
Kolkata -700032

Faculty of Engineering and Technology
JADAVPUR UNIVERSITY
Kolkata-700032

Certificate of Approval

The foregoing thesis titled, “**2RC MODEL BASED STATE OF CHARGE ESTIMATION OF LITHIUM-ION BATTERY**” is hereby approved as a creditable study of an Engineering subject carried out and presented in a manner satisfactory to warrant its acceptance as a pre-requisite to the degree of Master in Control System Engineering for which it has been submitted. It is understood that, by this approval, the undersigned does not necessarily endorse or approve any statement made, opinion expressed, or conclusion therein but approves this thesis only for the purpose for which it is submitted.

Final Examination for Evaluation of the Thesis

.....

.....

.....

Signature of the Examiners

Declaration of Originality

I hereby declare that this thesis contains a literature survey and original research Work by the undersigned candidate, as part of his Master in Control System Engineering curriculum. All information in this document has been obtained and Presented by academic rules and ethical conduct. I also declare as required by these rules and conduct, I have fully cited and referenced all material and results that are not original to this work.

Name: Ali Hossain Mondal

Examination Roll No.: M4CTL23002

Thesis Title: 2RC MODEL BASED STATE OF CHARGE
ESTIMATION OF LITHIUM-ION BATTERY.

Signature with Date:

ACKNOWLEDGEMENT

I sincerely thank my supervisor, Prof. Ranjit Kumar Barai, Department of Electrical Engineering, Jadavpur University, Kolkata, for his invaluable guidance, suggestions, encouragement, and constant support throughout my thesis work, which helped me in successfully completing it. It was a great honour for me to pursue my research under his supervision.

I would also like to thank all my classmates for their continuous help and support without which this would not have been possible.

I would like to express my gratitude towards all the staff of the control systems laboratory for providing constant encouragement throughout my thesis work.

Last but not least, I extend my words of gratitude to my parents, Mr. Kutubuddin Mondal and Mrs. Ammajan Mondal, my brother Mr. Imran Hossain Mondal, and my little sister Miss Rifatajmin Mondal for their endless love and support to guide me through every thick and thin of life.

Ali Hossain Mondal

M.E (Control System Engineering)

Department of Electrical Engineering

Jadavpur University, Kolkata – 700032

ABSTRACT

Safe reliable and efficient utilization management of rechargeable lithium-ion batteries relies on accurate real-time state-of-charge (SOC) estimation. Real-time estimation of the state of charge (SOC) of the battery is a crucial need in the growing fields of plug-in hybrid electric vehicles and smart grid applications. Model-based SOC observers have been widely used to estimate the SOC due to their high accuracy and robustness. The accuracy of the model used to characterize the battery's properties directly affects the estimation algorithm's accuracy. We employ a piecewise linear approximation with variable coefficients to represent the intrinsically nonlinear relationship between the open-circuit voltage (VOC) and the SOC of the battery, taking into account a resistance-capacitance (RC)–equivalent circuit to simulate the dynamics of the battery. Numerous experimental test results on lithium (Li)-polymer batteries demonstrate that the RC parameters also change in response to changes in the SOC and charging/discharging rates, in addition to the VOC–SOC relationship coefficients. The typical battery state-space model's observability matrix is ill-conditioned when the battery's slope from state-of-charge to open-circuit voltage (VOC) profile is near zero. Normally overlook this issue when we estimate the state of Charge and get unreliable SOC estimation. So choose the state carefully and resolve the observability problem. And model the battery parameter and thermal effect with the proper dependency of SOC and temperature (T). This article describes and analyzes the SOC estimation of both the conventional state space and new state space based on simulation.

CONTENTS

ABSTRACT.....	v
List of Abbreviations.....	ix
List of Figures.....	xi
Chapter 1: Introduction.....	1
1.1 Motivation.....	2
1.2. Thesis Scope and Objectives.....	3
Chapter 2: Literature Survey.....	4
2.1 Current and Future Energy Consumption.....	4
2.2 Overview of Battery Terminologies and Definitions.....	5
2.2.1 Rechargeable and Non-Rechargeable Battery Cells.....	5
2.2.2 Charge Rate (C-Rate)	6
2.2.3 Capacity or Nominal Capacity.....	6
2.2.4 Open-Circuit Voltage (OCV).....	6
2.2.5 Terminal Voltage (V_T).....	6
2.2.6 State of Charge (SOC).....	6
2.2.7 Cell, Modules and Packs.....	7
2.3 Battery modelling.....	8
2.3.1. Equivalent Circuit Models.....	8
2.3.2. Electrochemical Models.....	9
2.3.3. Thermal Management Systems.....	9

2.3.4. Behavioural Models.....	10
2.3.5 Parameter Identification.....	11
2.3.6 Model Validation.....	10
2.4 State of Charge Estimation.....	10
Chapter 3: Various Observers of SOC Estimator.....	12
3.1 SOC Definition.....	12
3.2 Coulomb Counting Method.....	13
3.3 Open-Circuit Voltage (OCV) Method.....	14
3.4 Fuzzy logic method.....	15
3.5 The Kalman Filter (KF) Method.....	16
3.6 The Extended Kalman Filter (EKF).....	18
3.7 The Unscented Kalman Filter (UKF).....	20
Chapter 4: Basic Aspects Model-Based SOC Estimation.....	26
4.1 Introduction.....	26
4.2 Empirical Models.....	26
4.3 Equivalent Circuit Models	27
4.3.1 Introduction.....	27
4.3.2 Rint Model.....	27
4.3.3 The Thevenin Model (1RC)	28
4.3.4 The Improved Thevenin Model (2RC)	30

Chapter 5: Implementation of Simulation Data-based Modeling.....	32
5.1 Introduction.....	32
5.2 V_{OC} -SOC Relationship.....	32
5.2.1 Piecewise linear mapping of V_{OC} -SOC curve.....	33
5.3 Battery Model Identification.....	34
5.3.1 Introduction.....	34
5.3.2 1RC Battery Modeling.....	36
5.3.3 High Fidelity Electrical Model.....	38
5.3.4 2RC Battery modeling.....	40
5.4 Observability check of the State Space Model.....	42
5.4.1 Proposed New State Space Model.....	44
5.5 Parameter Identification of the Battery Model.....	45
Chapter 6: SOC Estimation Using the Unscented Kalman Filter.....	50
6.1 Introduction.....	50
6.2 The Unscented Kalman Filter Algorithm.....	50
6.3 SOC estimation of the derived model.....	55
Chapter 7: Discussion and Conclusion	60
7.1 Comparative Study of Simulation.....	60
7.2 Discussion.....	64
7.3 Conclusion and Future work	65
Chapter 8: References.....	66

List of Abbreviations

OCV	: Open Circuit Voltage
SOC	: State of Charge
BMS	: Battery Management System
LQR	: Liner Quadratic Equation
ECM	: Electrical Circuit model
EV	: Electric Vehicle
HEV	: Hybrid Electrical Vehicle
μ C	: Microcontrollers
1D	: One Dimension
AC	: Alternative Current
Ah	: Ampere-hour
ANN	: Artificial Neural Networks
ASPO	: Association for the Study of Peak Oil and Gas
BEV	: Battery Electric Vehicles
EKF	: Extended Kalman Filter
KF	: Kalman Filter
Li-ion	: Lithium ion

LTI	: Linear Time Invariant
LTV	: Linear Time Varying
MSE	: Mean Square Error
OCV	: Open Circuit Voltage
ODE	: Ordinary Differential Equation
PDE	: Partial Differential Equation
PHEV	: Plug-in Hybrid Electrical Vehicles
RBS	: Regenerative Braking System
RMS	: Root Mean Square
ROM	: Reduced Order Model
SMC	: Sliding Mode Control

List of Figures

Figure 2.1 Imaginary State of Charge Gauge Indicator.....	7
Figure 2.2 Battery cell, module, and pack [20]	8
Figure 3.1 Voltage curves under different discharging current.....	15
Figure 4.1 Rint model structure.....	28
Figure 4.2 The Thevenin circuit model.....	29
Figure 4.3 2RC the Thevenin Model [8].....	30
Figure 5.1 SOC – V_{OC} carve of Battery charging [31].....	33
Figure 5.2 Piecewise linear mapping of VOC-SOC curve [1]	34
Figure 5.2 Input current pulse.....	35
Figure 5.3 Output voltage characteristics.....	35
Figure 5.4 1RC Battery Model [20]	36
Figure 5.5 ECM with SOC and T dependent [18]	38
Figure 5.6 Battery Simscape block model [18]	39
Figure 5.7 2RC Battery Model [2]	40
Figure 5.8 Plot of a_i vs SOC.....	43
Figure 5.9 Input current pulse.....	46
Figure 5.10 Output Voltage from Testing.....	47
Figure 5.11 ECM model in Simulink.....	47

Figure 5.12 Measurement and The Simulated value of voltage.....	48
Figure 5.13 Parameter estimation progress.....	49
Figure 5.14 Parameter estimation after 12 iterations.....	49
Figure 6.1 Electrical Equivalent Circuit Model (2RC)	56
Figure 6.2 State transition equation block.....	56
Figure 6.3 Measurement equation block.....	57
Figure 6.4 Simulink block of SOC estimation.....	58
Figure 6.5 SOC simulation data.....	59
Figure 7.1 current and voltage profile for Experiment.....	60
Figure 7.2 Temperature response plot.....	61
Figure 7.3 SOC Response and Estimation Error plot.....	61
Figure 7.4 SOC Error and the response of the new model.....	62
Figure 7.5 SOC response of conventional and new model.....	63
Figure 7.6 Error in SOC Estimation of different method.....	64

.....

Chapter 1

Introduction

Lithium-ion (Li-ion) batteries have become more and more commonplace in numerous applications that impact our daily lives, including digital cameras, laptops, cell phones, and other portable electronics, Electric vehicles, Smart grids, and Micro power grids, etc. In the last ten years, lithium-ion batteries have drawn more attention because of their high energy density, gradual loss of charge while not in use, and lack of hysteresis. These days, plug-in hybrid electrical vehicles (PHEVs) and second-generation hybrid electric vehicles (HEVs) also employ them. Accurate management, monitoring, and control procedures are required as battery applications and consumption grow in order to enhance the battery packs' performance, efficiency, safety, dependability, and durability. Particularly when it comes to electrical and hybrid cars Because unexpected acceleration or regenerative braking system movements force the battery operating conditions to rapid transients and frequent cycles of charging and discharging at this time battery management systems (BMS) are essential. Battery Management Systems (BMS) must be able to provide an accurate real-time estimate for the Battery State of Charge (SOC). The primary problem with SOC is that it cannot be quantified, necessitating methods for estimating states and parameters.

A traditional state-space model is usually derived with the SOC as one of the states that need to be monitored in order to estimate the battery's

state of charge (SOC) using the ECM [2]. Many SOC estimate strategies based on the traditional state-space model have been proposed by researchers. The majority of their efforts have been focused on increasing the accuracy of the SOC estimation by using different online parameter identification techniques, including the Kalman filter [34], recursive least square [35], Autoregressive-moving-average model [36], etc. In order to improve SOC estimation, more advanced observers such as the Luenberger observer, sliding mode observer [38], extended Kalman filter [22], unscented Kalman filter [29], H-infinity filter [37], etc., can be used. This will help proactively capture battery nonlinearities and degradation [19]. The impairment of battery ECM observability, a fundamental problem that is often disregarded, results in poor SOC estimation accuracy in the range of flat SOC- V_{OC} profiles [26]. A state-space model is proposed to fundamentally solve the ill-conditioned observability issue, [20]. A comparative study on this topic is discussed in this thesis.

1.1 Motivation

The global need to employ clean and renewable energy sources and cut emissions is what spurs this research. This study takes into account two crucial factors for hybrid and electric cars: energy storage and battery management. A fluid level sensor in a typical car makes it easy to determine how much gasoline is left in the tank. Measuring the amount of useable energy remaining, or SOC, in electric vehicles can be challenging. This particularly applies to situations where the driving cycle causes the battery to experience rapid transients in terms of charging and discharging. A precise mathematical model and a

reliable estimating method are required because SOC cannot be measured.

The battery's remaining useful life, or RUL is a crucial factor to take into account when buying an electric car. In order to increase battery life and remain useful Life, proper battery operation and management are crucial. Frequently employed are model-based tactics.

1.2 Thesis Scope and Objectives

In this thesis, different battery modelling techniques and SOC estimation strategies are considered and compared with respect to their performances. Lithium-ion battery cell models are selected, refined, implemented, and validated using measured and simulated test data. Comparative study of different state space models of lithium-ion batteries and selection of the efficient and effective ways of SOC estimation to build a good Battery management system.

Chapter 2

Literature Survey

The estimation of State of Charge (SOC) in batteries is a fundamental aspect of battery management systems in various applications, including electric vehicles, portable electronics, renewable energy storage, and more. SOC refers to the measure of how much energy a battery contains relative to its fully charged state. Accurate SOC and SOH estimation is essential for optimizing battery performance, ensuring safe operation, and prolonging battery life.

2.1 Current and Future Energy Consumption

For our energy needs today, our societies mainly rely on fossil fuels like coal and oil. However, due to concerns about these energy sources' effects on the environment, economy, and geopolitics, there is widespread concern about them. Although fossil fuels are created naturally, there is a strain on available reserves because of the faster rate of consumption than production. As demonstrated by the Association for the Study of Peak Oil and Gas (ASPO), which projects that the oil extraction peak will be reached before 2020 excessive reliance on fossil fuels is unsustainable and the reserves are depleting quickly. Consequently, it is imperative to take into account alternate energy sources, especially electrification.

Electrochemical batteries are necessary for energy storage, which is a prerequisite for electrification. In every industry (automotive, aerospace, medical, military, etc.) and consumer product (e.g., low current applications, household appliances, cell phones, and laptop computers), they are commonly employed to convert chemical energy to electrical energy. An essential component of electric and hybrid cars is batteries. Particularly intriguing are lithium-based batteries because of their great energy density. In addition, they are less hazardous than lead acid or nickel-cadmium cells and may be recycled after use, which reduces the environmental impact.

2.2 Overview of Battery Terminologies and Definitions

Understanding battery terminology and definitions is essential for effectively working with batteries, whether in everyday applications like smartphones or more complex systems such as electric vehicles and renewable energy storage. Here's an overview of key battery terminologies and their definitions:

2.2.1 Rechargeable and Non-Rechargeable Battery Cells

A battery is referred to as the primary battery if it is incapable of being recharged by irreversible chemical reactions. A second battery is referred to as the secondary battery if it permits reversible chemical reactions, indicating that it is a rechargeable battery [29].

2.2.2 Charge Rate (C-Rate)

The rate at which a battery is charged or drained about its maximum capacity is known as the battery charge rate or C-rate. With a 1C rate, a completely charged battery will be discharged in one hour by the applied discharge current. This corresponds to a discharge current of 20 amps for a battery with a capacity of 20 amp-hours. For this battery, a C/2 rate would be $20/2 = 10$ Amps and a 5C rate would be $20 \times 5 = 100$ Amps.

2.2.3 Capacity or Nominal Capacity

The total Amp-hours that a battery can hold when fully discharged from 100% state-of-charge to its rated minimum cut-off voltage at a specific discharge current (referred to as a C-rate) is known as its coulometric capacity. The discharge current (measured in amps) multiplied by the discharge time (measured in hours) yields the capacity [29].

2.2.4 Open-Circuit Voltage (OCV)

The voltage across a battery when no current is flowing. It is a valuable indicator of a battery's SOC.

2.2.5 Terminal Voltage (V_T)

The voltage measured between the battery terminals when a load is applied

2.2.6 State of Charge (SOC)

The State of Charge (SOC), which displays the battery's current capacity as a percentage of its potential capacity, is an important indicator for electric vehicles. As a result, it offers a measurement of the electrical energy that a battery can hold. It is comparable to a

gasoline gauge on a car with a traditional internal combustion engine. State of Charge (SOC) is a dimensionless percentage that ranges from 0% to 100%. It is important to note that a zero SOC does not indicate that the battery is completely empty; rather, it indicates that further discharge of the battery is no longer possible without resulting in irreversible chemical reactions and irreparable damage to the battery [30].

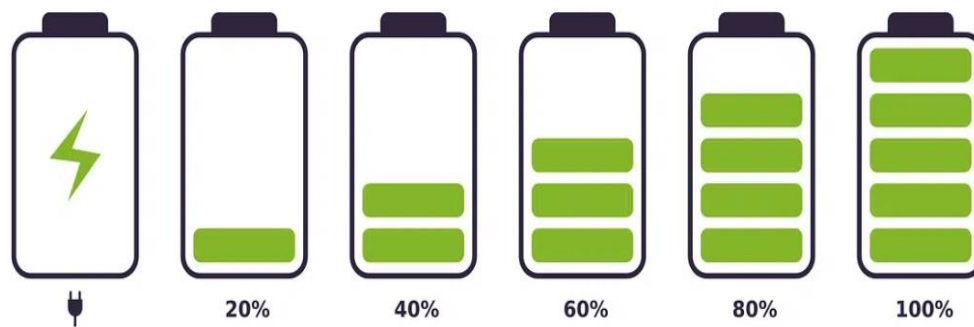


Figure 2.1 Imaginary State of Charge Gauge Indicator

2.2.7 Cell, Modules and Packs

The high-voltage battery pack found in all hybrid electric vehicles (HEVs), plug-in hybrid electric vehicles (PHEVs), and electric vehicles (EVs) is made up of two or more modules, each of which has two or more cells. The smallest element that can be joined in series or parallel to form a single module is called a cell. After that, a module is linked in either a parallel or series configuration to create a single pack.

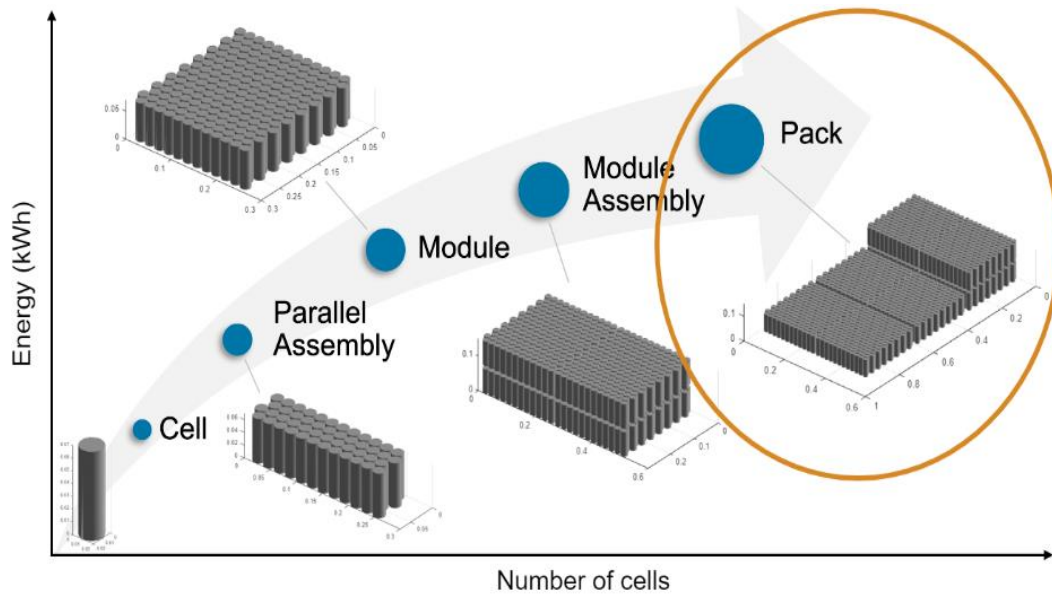


Figure 2.2 Battery cell, module, and pack [20]

2.3 Battery Modeling

Battery modeling is an important and challenging consideration in battery management systems. Battery modeling refers to the process of creating mathematical or computational representations of battery behavior, characteristics, and performance. These models are essential for understanding, analyzing, and predicting how batteries will perform in various applications. There are different types of battery models, ranging from simple equivalent circuit models to complex electrochemical models. Here is an overview of battery modeling:

2.3.1. Equivalent Circuit Models

Equivalent circuit models are simple electrical circuit representations of a battery [18]. They consist of resistors, capacitors, and voltage

sources that emulate the various electrical and electrochemical processes within the battery. Common models include:

Thevenin Model: A basic model consisting of a voltage source and a resistor and a more complex Thevenin model when Resistance with RC parallel components is present.

Randles Model: a more complex model that includes additional components to account for electrochemical behavior.

2.3.2. Electrochemical Models

Electrochemical models provide a more detailed representation of the physical and chemical processes occurring within a battery. They consider parameters such as diffusion, reaction kinetics, and ion transport [31].

2.3.3. Thermal Management Systems

One crucial factor to take into account with lithium ion batteries is thermal control. Unwanted repercussions could arise from unsafe operation circumstances caused by battery overheating or thermal runaways [46]. To maintain the battery within the intended operating range It is necessary to measure and keep an eye on the cell core's temperature. Since temperature is difficult to measure, an estimate of the temperature is required. Rechargeable models may be combined with thermal models to provide a more complete method for characterizing the performance of batteries [45].

Thermal models are used to simulate the temperature distribution within a battery, as temperature significantly affects battery performance and safety. These models often work in conjunction with

electrochemical models to account for heat generation and dissipation [2].

2.3.4 Behavioral Models

Behavioral models focus on the external behavior of a battery rather than the internal processes. They are often used in system-level simulations to assess how batteries interact with other components in a larger system.

2.3.5 Parameter Identification

Parameter identification is the most important part of Battery modeling [1]. Accurate modeling requires determining the model's parameters. Parameter identification involves measuring or estimating values for various model parameters, such as resistance, capacity, rate constants, and voltage which are also the function of SOC and the temperature of the cell [18].

2.3.6 Model Validation

Model validation is crucial to ensure that the model accurately represents the real-world behavior of the battery. It involves comparing model predictions to experimental data and making adjustments if necessary. With the help of Recorded experimental data, the model was verified in MATLAB Simulink experiment [9].

2.4 State of Charge Estimation

This thesis demonstrates the State of Charge (SOC) estimation process, which is the most important part of a Battery management system. SOC estimation is the process of determining the current charge level of a battery relative to its maximum capacity. Of the

different approaches to SOC estimation, coulomb counting (Ah counting) [39] is the most conventional method. Conversely, there is also the option to measure the open-circuit voltage (VOC) alone [34] or in conjunction with coulomb counting but this method is inappropriate for online SOC estimation. The SOC cannot be directly measured That's which observer based is why observer-based techniques, such as the Kalman filter [29], the sliding mode [35], or H^∞ [36], have been developed and have become popular recently to compensate for the overpotential dynamics of the battery and to calculate the SOC based on the estimated VOC.

Chapter 3

Various Observers of SOC Estimation

3.1 SOC Definition

The SOC is a significant indicator for lithium-ion battery management since it allows users and battery management systems (BMS) to monitor and control the battery's operation. Accurate SOC estimation is critical for improving battery performance, increasing battery life, and assuring safe and dependable operation in a wide range of applications, including electric Vehicle(EV), smart-grid, and renewable energy systems.

The SOC for a lithium-ion battery is a measure of the current available capacity or energy level within the battery as a percentage of its fully charged capacity. It indicates how much of the battery's total charge has been used or how much capacity remains. SOC is typically expressed as a percentage, where 0% represents a fully depleted battery, and 100% signifies a fully charged battery.

$$SOC = \frac{Q_{remain}}{Q_{rated}} \times 100 \% \quad (3.1)$$

Where,

Q_{remain} is the remaining capacity of the battery.

Q_{rated} is the rated capacity of the battery.

SOC estimation is a critical aspect of managing and controlling battery systems, particularly in applications like electric vehicles, renewable energy storage, and portable electronics. Various observers and estimation techniques are used to estimate SOC accurately. Here, we will discuss several of them.

3.2 Coulomb Counting Method

Coulomb counting is a widely used method for estimating the SOC in lithium-ion batteries. This method calculates the SOC by keeping track of the electric charge that flows into or out of the battery during charging and discharging. It is also known as the current integration or ampere-hour method, it can estimate real-time SOC based on the last SOC status, involving measuring the charge and discharging currents of a battery and integrating them over time to determine SOC.

$$SOC(t) = f(i_L, Q_{av}) = SOC(t_0) + \frac{1}{Q_{av}} \int_{t_0}^{t_1} i_L dt \quad (3.2)$$

Where,

$SOC(t_0)$ is the initial state of charge.

$SOC(t)$ is the real-time State of Charge.

Q_{av} is the Available Capacity.

i_L is real-time discharge current.

Specific factors, such as temperature, battery history, charge and discharge cycles, and others, affect the coulomb counting method. Additionally, accurate SOC is heavily dependent on accurate initial SOC and capacity. The calculated SOC may be offset if the initial SOC

and its capacity are not correlated. Due to integration, which results in the discrepancy between the calculated SOC and the true SOC, the inaccurate current value may accumulate over time. Furthermore, the self-discharge or parasitic reactions in the battery are not taken into account by the coulomb counting approach. The SOC can be reset to fix this flaw. Also, it is impossible to use when the battery is working in a dynamic environment coulomb counting approach. The SOC can be reset to fix this flaw.

3.3 Open-Circuit Voltage (OCV) Method

The Open-Circuit Voltage (OCV) method is a simple and widely used technique for estimating the SOC of a battery. It relies on the relationship between the battery's open-circuit voltage and its state of charge. The basic idea is to measure the voltage of the battery when it is not delivering or receiving any current (i.e., under open-circuit conditions) and then use this voltage to estimate the SOC. However, the accurate OCV only can be measured after the battery rests for a long time. If the rated voltage of the lithium-ion battery is 3.7V, the OCV varies less than 1 V during operation. Especially, the OCV has only changed 0.3 V when SOC is between 0.4~0.7, this makes the SOC estimation difficult [25]. The open circuit voltage method cannot effectively estimate the state of charge in real time due to the primary drawback of the battery, which is the lengthy rest period required to acquire accurate OCV. An example of equilibrium potential versus SOC curves is presented in Figure 3.1. The lithium-ion battery is tested under an actual load, with the battery being discharged from full

charge to 0% of SOC at constant currents of 0.25 Coulomb Ampere (C A), 0.5 C A, and 1 C A, respectively, in the real-world environment.

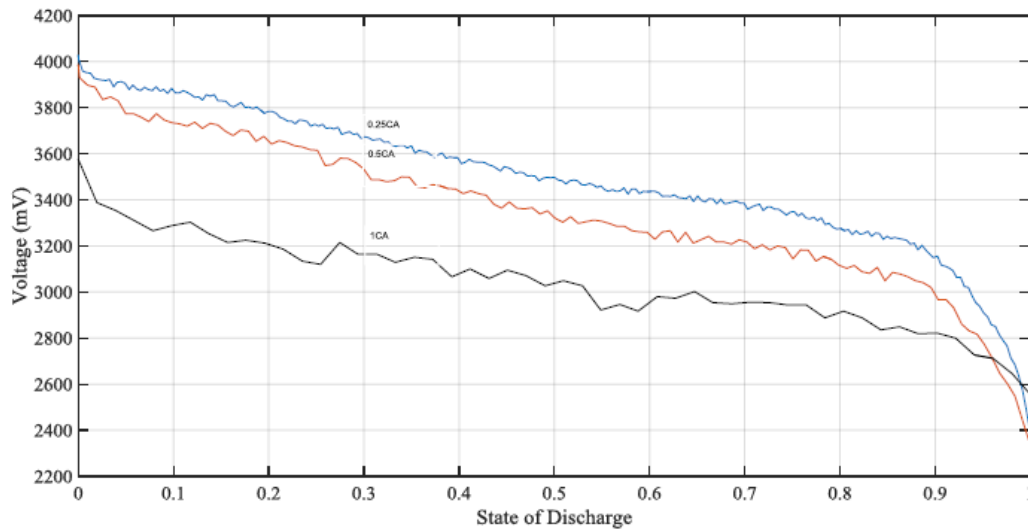


Figure 3.1 Voltage curves under different discharging current

Battery internal material will be depleted and fade after multiple cycles of charging and discharging. The battery will experience a significant reduction in real capacity during hundreds of charge-discharge cycles.

3.4 Fuzzy logic method

SOC of battery systems has been devised and validated for many systems in [25]. The technique comprises the analysis of data generated by Coulomb counting and/or impedance spectroscopy techniques using fuzzy logic models. A method for estimating SOC of lithium-ion batteries using fuzzy logic has been developed [26] and may find application in portable defibrillators. The measurements of voltage recovery and ac impedance have been completed, and they are the input parameters used by the fuzzy logic model.

By monitoring the impedance at three frequencies, Singh et al. [27] presented an estimating system that can choose attributes from a database to create fuzzy logic models for available capacity and SOC estimation. An enhanced Coulomb metric approach is used in [28] to estimate the SOC, and a learning system is used to correct for the time-dependent variance. The learning system adjusts the Coulomb metric technique such that the time-dependent fluctuation in the estimation process does not introduce errors. The suggested learning system makes use of fuzzy logic models, which function as a learning system component rather than being employed for SOC estimation.

3.5 The Kalman Filter Method (KF)

The Kalman filter was first proposed in 1960 by mathematician R.E. Kalman. One algorithm that can be used for the linear system is the Kalman filter. The intended signal and data can be recovered based on the observation state by estimating the model's observation state using minimum variance. The Kalman filter heavily relies on the system model during battery estimate. The SOC divergence is caused by the system model's mistake. The preceding issue—that the Kalman filter is only appropriate for linear systems—was recently addressed with the proposal of the extended Kalman filter. The extended Kalman filter estimates the system's observed state by first applying the first-order Taylor series expansion to the non-linear equation. Converting a nonlinear system to a linear system is the basic goal of the extended Kalman filter [27]. Use a minimum variance filter to process the data once the system has been linearized. The study builds measurement

and observation equations before estimating the SOC using the extended Kalman filter. The extended Kalman filter is heavily dependent on the accuracy of the model, just like the Kalman filter.

State-space model

$$x_{k+1} = A_k x_k + B_k u_k + w_k \quad (3.3)$$

$$y_k = C_k x_k + v_k \quad (3.4)$$

Where w_k and v_k are independent, zero-mean, Gaussian noise processes of covariance matrices Σ_w and, Σ_v respectively.

Initialization: For $k = 0$, set

$$\hat{x}_0(+) = E[x_0] \quad (3.4)$$

$$\Sigma_{x_0}(+) = E[(x_0 - E[x_0])(x_0 - E[x_0])^T] \quad (3.5)$$

Computation for $k = 1, 2, \dots$

State estimate propagation

$$\hat{X}_k(-) = A_{k-1} \hat{X}_{k-1}(+) + B_{k-1} u_{k-1} \quad (3.6)$$

The Kalman gain matrix

$$L_k = \Sigma_{e,k}(-) C_k^T [C_k \Sigma_{e,k}(-) C_k^T + \Sigma_V]^{-1} \quad (3.7)$$

State estimate update

$$\hat{x}_k(+) = \hat{x}_k(-) + L_k [c_k \hat{x}_k(-)] \quad (3.8)$$

After initialization, the Kalman filter repeats two actions. Initially, it forecasts the error covariance, system output, and the value of the subsequent state. Second, it adjusts the estimate of the current condition using a measurement of the system output. The error covariance estimates and the projected state are represented by the symbols $\hat{x}_k(-)$ and $\Sigma_{e,k}(-)$, respectively, at time index k but before the measurement. After the measurement, the adjusted estimations are indicated by $\hat{x}_k(+)$ and $\Sigma_{e,k}(+)$.

The prediction step is accomplished by propagating the system input through the system dynamics

$$\hat{x}_{k+1}(-) = A_k \hat{x}_k(+) + B_k u_k \quad (3.9)$$

The state uncertainty also update

$$\Sigma_{e,k+1}(-) = A_k \Sigma_{e,k}(+) A_k^T + \Sigma_w \quad (3.10)$$

The state uncertainty also decreased due to the new information provided. The assumption that the noise processes are white is rarely met in practical applications. If this assumption is violated the Kalman filter will not be optimal and can become unstable [44].

3.6 The Extended Kalman Filter (EKF)

The Extended Kalman Filter must be applied to non-linear systems. The system model in the EKF is linearized around the present estimate of the a priori state. The Kalman gain is then computed using the linearized model. When dealing with non-linear systems.

Let,

$$x_{k+1} = f(x_k, u_k) + w_k \quad (3.11)$$

$$y_k = g(x_k, u_k) + v_k \quad (3.12)$$

It is assumed that both w_k and v_k are white noise, with zero mean and known covariance matrices (Q) and (R), respectively. The state equation (3.16) is represented by the first equation and the output equation (3.17) by the second equation.

The system model is used to obtain the a priori estimates in a manner similar to that of the Kalman filter, which is as follows in this instance

$$\hat{x}_{k+1|k} = f(\hat{x}_{k|k}, u_k) \quad (3.13)$$

$$P_{k+1|k} = F_k P_{k|k} F_k^T + Q_k \quad (3.14)$$

The system models are then linearized around $\hat{x}_{k+1|k}$ such that

$$F_k = \left. \frac{\partial f(x_k, u_k)}{\partial x_k} \right|_{x_k = \hat{x}_{k+1|k}} \quad (3.15)$$

$$H_k = \left. \frac{\partial g(x_k, u_k)}{\partial x_k} \right|_{x_k = \hat{x}_{k+1|k}} \quad (3.16)$$

The Kalman gain K_{k+1} is then calculated using the linearized model such that,

$$K_{k+1} = P_{k+1|k} G_{k+1}^T (G_{k+1} P_{k+1|k} G_{k+1}^T + R_{k+1})^{-1} \quad (3.17)$$

A posteriori estimates are then obtained as

$$\hat{x}_{k+1|k+1} = \hat{x}_{k+1|k} + K_{k+1} (Z_{k+1} - g(\hat{x}_{k+1|k}, u_k)) \quad (3.18)$$

$$P_{k+1|k+1} = (1 - K_{k+1}G_{k+1})P_{k+1|k} \quad (3.19)$$

When uncertainties are present, the linearization of the extended Kalman filter may become unstable. The Smooth Variable Structure Filter is a more reliable estimation technique for battery condition monitoring (SVSF).

3.7 The Unscented Kalman Filter (UKF)

The state transition and measurement equations for an M-state discrete-time nonlinear system have additive process and measurement noise terms with zero mean and covariances Q and R, respectively:

$$x[k + 1] = f(x[k], u_s[k] + w[k] \quad (3.20)$$

$$y[k] = h(x[k], u_m[k] + v[k] \quad (3.21)$$

$$w[k] \sim (0, Q[k]) \quad (3.22)$$

$$v[k] \sim (0, R[k]) \quad (3.23)$$

Initially provide Q as process noise and R as measurement noise.

1) Determine the initial value $x[0]$ of the state variable and the initial covariance matrix p .

$$\hat{x}[0|-1] = E(x[0]) \quad (3.24)$$

$$P[0|-1] = E(x[0] - \hat{x}[0|-1])(x[0] - \hat{x}[0|-1])^T \quad (3.25)$$

Here

\hat{x} is the state estimate and $\hat{x}[k_a | k_b]$ denotes the state estimate at time step k_a using measurements at time steps $0, 1, \dots, k_b$. So $\hat{x}[0|-1]$ is the best guess of the state value before you make any measurements. You specify this value when you construct the filter.

2) For each time step k , update the state and state estimation error covariance using the measured data, $y[k]$. In the software, the correct command performs this update.

i) Choose the sigma points $\hat{x}^{(i)}[k | k - 1]$ at time step k .

$$\hat{x}^{(0)}[k | k - 1] = x[k | k - 1] \quad (3.26)$$

$$\hat{x}^{(i)}[k | k - 1] = x[k | k - 1] + \Delta x^{(i)}, \quad i = 1, \dots, 2M \quad (3.27)$$

$$\Delta x^{(i)} = (\sqrt{c^P[k | k - 1]})^T i \quad i = 1, \dots, M \quad (3.28)$$

$$\Delta x^{(M+i)} = -(\sqrt{c^P[k | k - 1]})^T i, \quad i = 1, \dots, M \quad (3.39)$$

Where

$c = \alpha^2(M + k)$ is a scaling factor.

$\sqrt{c^P}$ is the Matrix square root of c^P .

ii) Use the nonlinear measurement function to compute the predicted measurements for each of the sigma points.

$$\hat{y}^{(i)}[k | k - 1] = h(\hat{x}^{(i)}[k | k - 1], u_m[k]) \quad i = 0, 1, \dots, 2M \quad (3.40)$$

iii) Combine the predicted measurements to obtain the predicted measurement at time k.

$$\hat{y}[k] = \sum_{i=0}^{2M} W_M^{(i)} \hat{y}^{(i)}[k | k - 1] \quad (3.41)$$

$$W_M^{(0)} = 1 - \frac{M}{\alpha^2(M+k)} \quad (3.42)$$

$$W_M^i = \frac{M}{2\alpha^2(M+k)} \quad i = 1, 2, \dots, 2M \quad (3.43)$$

iv) Estimate the covariance of the predicted measurement. Add $R[k]$ to account for the additive measurement noise.

$$p_y = \sum_{i=0}^{2M} W_c^{(i)} \hat{y}^{(i)}[k | k - 1] - \hat{y}[k] (\hat{y}^{(i)}[k | k - 1] - \hat{y}[k])^T + R[k] \quad (3.44)$$

$$w_c^{(0)} = (2 + \alpha^2 + \beta) - \frac{M}{\alpha^2(M+k)} \quad (3.45)$$

$$w_C^i = \frac{1}{2\alpha^2(M+k)} \quad i = 1, 2, \dots, 2M \quad (3.46)$$

v) Estimate the cross-covariance between $\hat{x}[k|k-1]$ and $\hat{x}[k]$

$$P_{xy} = \frac{M}{2\alpha^2(M+k)} \sum_{i=0}^{2M} (\hat{x}^{(i)}[k|k-1] - \hat{x}[k|k-1])(\hat{y}^{(i)}[k|k-1] - \hat{y}[k]^T) \quad (3.47)$$

The summation starts from $i = 1$ because

$$\hat{x}^{(0)}[k|k-1] - \hat{x}[k|k-1] = 0 \quad (3.48)$$

vi) Obtain the estimated state and state estimation error covariance at time step k .

$$K = P_{xy}P_y^{-1} \quad (3.49)$$

$$\hat{x}[k|k] = \hat{x}[k|k-1] + K(y[k] - \hat{y}[k]) \quad (3.50)$$

$$P[k|k] = P[k|k-1] - KP_yK_k^T \quad (3.51)$$

Where K is the the Kalman gain.

3) Predict the state and state estimation error covariance at the next time step.

i) Choose the sigma points $\hat{x}^{(i)}[k|k]$ at time step k .

$$\hat{x}^{(0)}[k|k] = \hat{x}[k|k] \quad (3.52)$$

$$\hat{x}^{(i)}[k|k] = \hat{x}[k|k] + \Delta x^{(i)} \quad i = 1, 2, \dots, 2M \quad (3.53)$$

$$\Delta x^{(i)} = (\sqrt{cP[k|k]})i \quad i = 1, \dots, M$$

$$\Delta x^{(M+i)} = -(\sqrt{cP[k|k]})i \quad i = 1, \dots, M$$

ii) Use the nonlinear state transition function to compute the predicted states for each of the sigma points.

$$\hat{x}^{(i)}[k+1|k] = f(\hat{x}^{(i)}[k|k], u_s[k]) \quad (3.54)$$

iii) Combine the predicted states to obtain the predicted states at time k+1.

$$\hat{x}[k+1|k] = \sum_{i=0}^{2M} W_M^{(i)} \hat{x}^{(i)}[k+1|k] \quad (3.55)$$

$$W_M^{(0)} = 1 - \frac{M}{\alpha^2(M+k)} \quad (3.56)$$

$$W_M^i = \frac{M}{2\alpha^2(M+k)} \quad i = 1, 2, \dots, 2M \quad (3.57)$$

iv) Compute the covariance of the predicted state. Add Q[k] to account for the additive process noise

$$P[k+1|k] = \sum_{i=0}^{2M} W_c^{(i)} (\hat{x}^{(i)}[k+1|k] - \hat{x}[k+1|k])(\hat{x}^{(i)}[k+1|k] - \hat{x}[k+1|k])^T + Q[k] \quad (3.58)$$

$$W_c^{(0)} = (2 - \alpha^2 + \beta) - \frac{M}{\alpha^2(M+k)} \quad (3.59)$$

$$W_c^i = \frac{1}{2\alpha^2(M+k)} \quad i = 1, 2, \dots, 2M \quad (3.60)$$

The previous algorithm is implemented assuming additive noise terms in the state transition and measurement equations [22].

Chapter 4

Basic Aspects of Model-Based SOC Estimation

4.1 Introduction

Modeling lithium-ion batteries involves capturing the electrochemical and physical processes that occur within the battery during charging and discharging. Several approaches can be taken, ranging from simple empirical models to more complex physics-based models. Here, I'll outline a general overview of lithium-ion battery modeling and mention some common models used in the field

4.2 Empirical Models

Empirical models are a type of mathematical model derived from experimental data without necessarily considering the underlying physical or chemical processes [15]. These models are based on observed relationships between input and output variables. While they lack a theoretical foundation, empirical models are often practical and useful, especially when a detailed understanding of the underlying mechanisms is not necessary or when the processes are too complex to be represented by theoretical equations.

4.3 Equivalent Circuit Models

4.3.1 Introduction

Equivalent circuit models are widely used to represent the electrical characteristics of batteries. These models simplify the complex electrochemical processes within a battery into a set of electrical components. The most common equivalent circuit models include the Thevenin model and the Randles circuit, which are often used to describe the behavior of batteries during charge and discharge cycles. Here's an overview of these models.

4.3.2 Rint model

The Rint (internal resistance) model is a simplified representation of the internal resistance of a battery. Internal resistance is a crucial parameter in battery modeling as it affects the voltage drop and power dissipation within the battery during charge and discharge cycles. Rint model structure is depicted in Figure 4.1 [13]. The Rint model has a straightforward structure U_L is the terminal voltage, and R_0 is the battery's internal resistance. The polarization reaction of the battery during the charge/discharge process cannot be represented by a Rint model. In the Rint model, the battery is composed of a resistance and an ideal voltage source (U_{OC}).

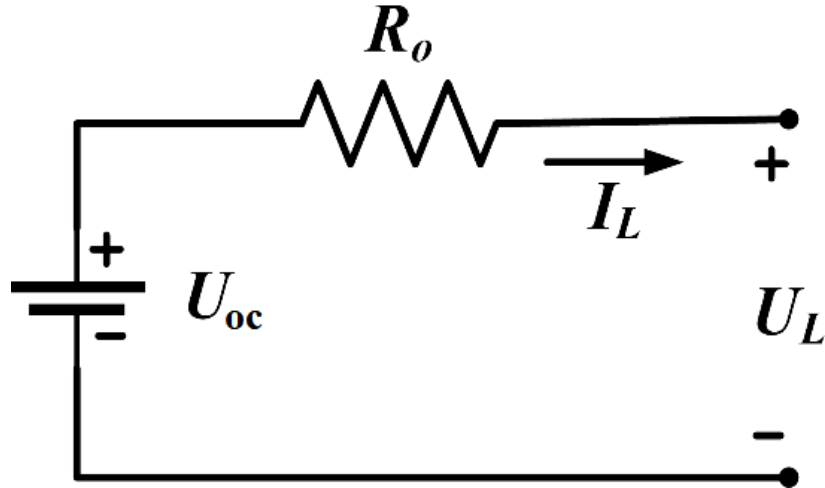


Figure 4.1 Rint model structure

4.3.3 Thevenin Model

A Thevenin model was created to address the issue that the Rint model was unable to accurately capture the polarization reaction [15]. The Thevenin model structure is depicted in Figure 4.2. The Thevenin model takes into account the polarization resistance R_1 and polarization capacitor C_1 in comparison to the Rint model. Where $I(t)$ is the charge/discharge current and V_1 is the voltage across the capacitance. The battery model is more accurate because of the additional resistance and pair of capacitors. Thevenin can precisely estimate the SOC of the battery when the battery charges/discharges in the stable state, which usually happens from 0.2 SOC to 0.8 SOC.

Thevenin circuit model

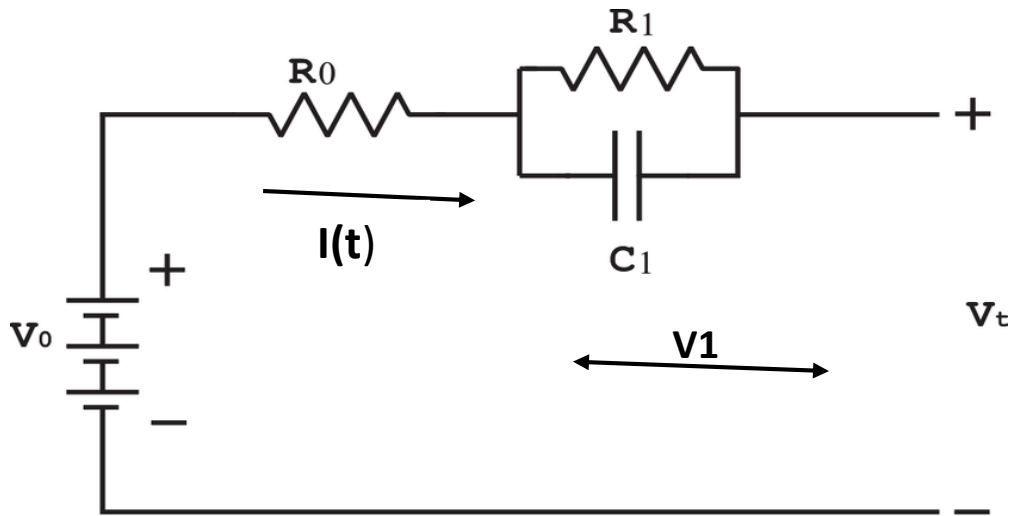


Figure 4.2 The Thevenin circuit model

The electrical behavior of the Thevenin model can be expressed as follows,

$$\frac{dv_1}{dt} = -\frac{v_1}{R_1 C_1} + \frac{I(t)}{C_1} \quad (4.1)$$

$$V_t = V_0(SOC) - R_0 I(t) - V_1(t) \quad (4.2)$$

4.3.4 Improved Thevenin Model (2RC)

The internal battery is a complicated process involving battery temperature, current intensity, battery health, and more unpredictable factors. The SOC of the battery shows strong nonlinear characteristics at the beginning and end of the charge/discharge operation [16]. To estimate the SOC more accurately, the Improved Thevenin model is considered. Figure 4.3 shows the second-order Thevenin model that adds another RC branch to the Thevenin model. In Figure 4.3, C_2 and R_2 are concentration polarization capacitance and concentration polarization resistance respectively. V_2 is the voltage across the concentration polarization capacitance.

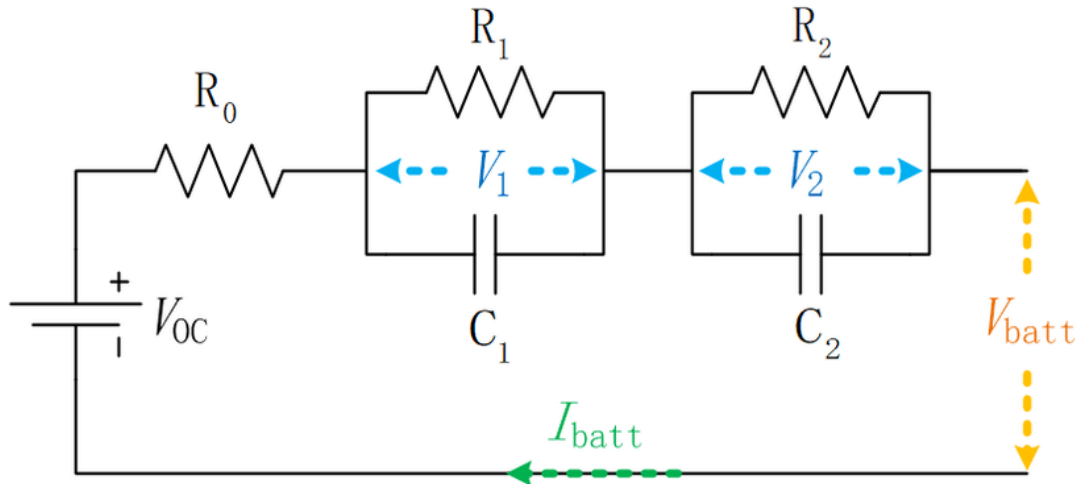


Figure 4.3 2RC the Thevenin Model [8]

The mathematic expressions of the second-order model are represented as follows

$$\frac{dv_1}{dt} = -\frac{v_1}{R_1C_1} + \frac{I(t)}{C_1} \quad (4.3)$$

$$\frac{dv_2}{dt} = -\frac{v_2}{R_2C_2} + \frac{I(t)}{C_2} \quad (4.4)$$

$$V_{Batt} = V_{oc}(SOC) - R_0I(t) - V_1(t) - V_2(t) \quad (4.5)$$

Chapter 5

Implementation of Simulation data-based Modeling

5.1 Introduction

For the SOC, estimation of a battery accurate battery modeling plays a very important role. There are several nonlinearities and uncertainties present in the lithium-ion Battery. The parameters of the Battery are dependent on the SOC, Temperature, input current other things. The Electrical Circuit Model (ECM) which includes the RC component is good for estimating the SOC. The State Space model is derived from the ECM model and we check the observability issue also. Using the MATLAB Physical test data set for battery modelling as an experimental dataset.

5.2 V_{OC} -SOC Relationship

The open Circuit Voltage (V_{OC}) of the lithium-ion Battery is a function of the State of Charge (SOC). The static relationship between V_{OC} and the SOC is intrinsically nonlinear shown in Figure 5.1. The nonlinearity of the model increases the complexity of the stability and performance analysis of the SOC estimators. The relationship is

determined by the materials used in the anode, cathode, and electrolyte in the battery [17].

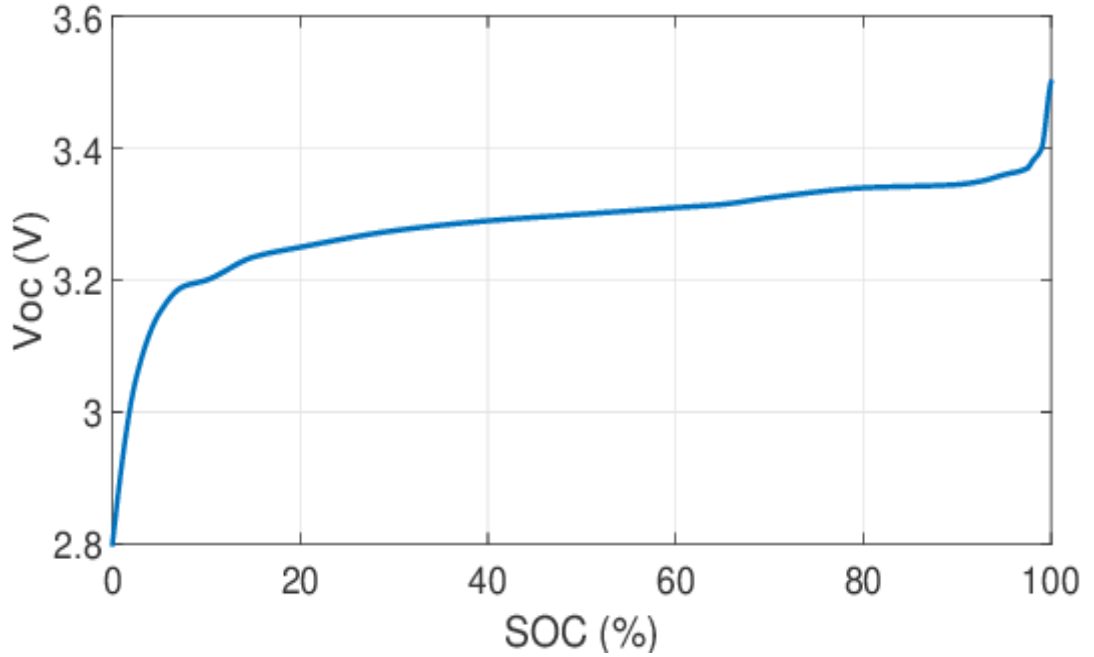


Figure 5.1 SOC – V_{oc} curve of Battery charging [31]

5.2.1 Piecewise linear mapping of V_{oc}-SOC curve

The static relationship between V_{oc} and the SOC is inherently nonlinear, despite the straightforward linear model for the battery. Piecewise linear mapping of the V_{oc}-SOC curve takes in different temperatures taking into account the Li-polymer battery's V_{oc}–SOC curve based on experimental findings, we demonstrate in [19]. we can describe the liner equation. Piecewise linear mapping of VOC-SOC curve shown in the figure 5.2.

$$V_{oc} = f(SOC) = b_0 + a_1 SOC \quad (5.2.1)$$

Where

a_1 is the slope of the V_{oc}–SOC curve.

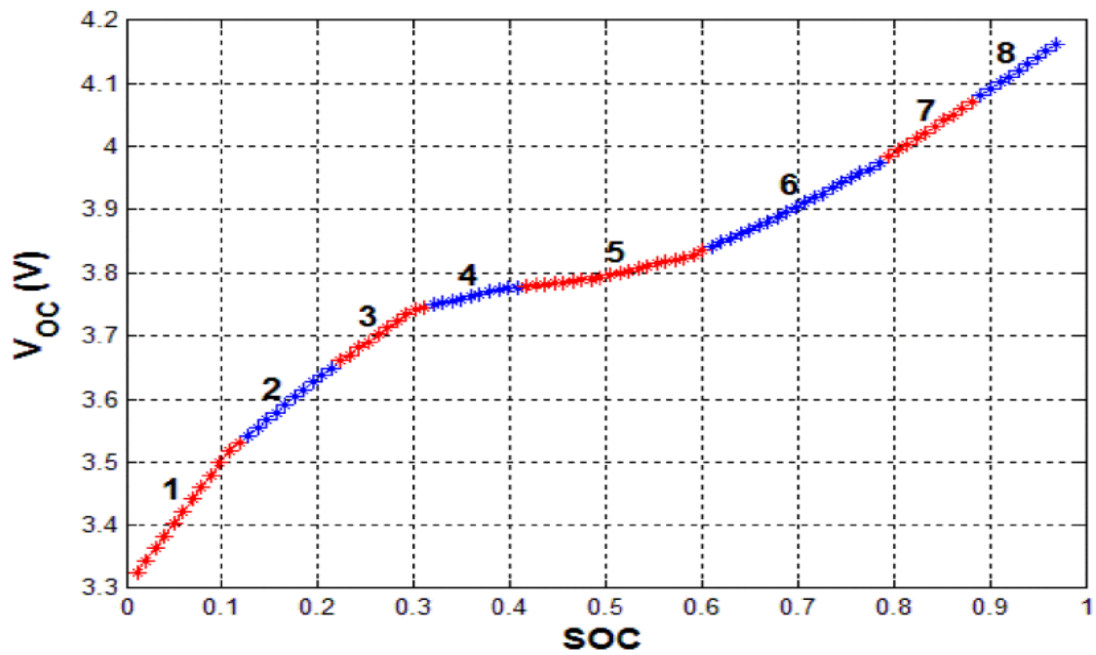


Figure 5.2 Piecewise linear mapping of VOC-SOC curve [1]

5.3 Battery Model Identification

5.3.1 Introduction

In a lithium-ion battery, if we give a current pulse Figure 5.2, it produces the output voltage characteristics shown in Figure 5.3. This output graph shows that there are nonlinearities present in the output plot. A sudden voltage drop at the initial and then a delayed response.

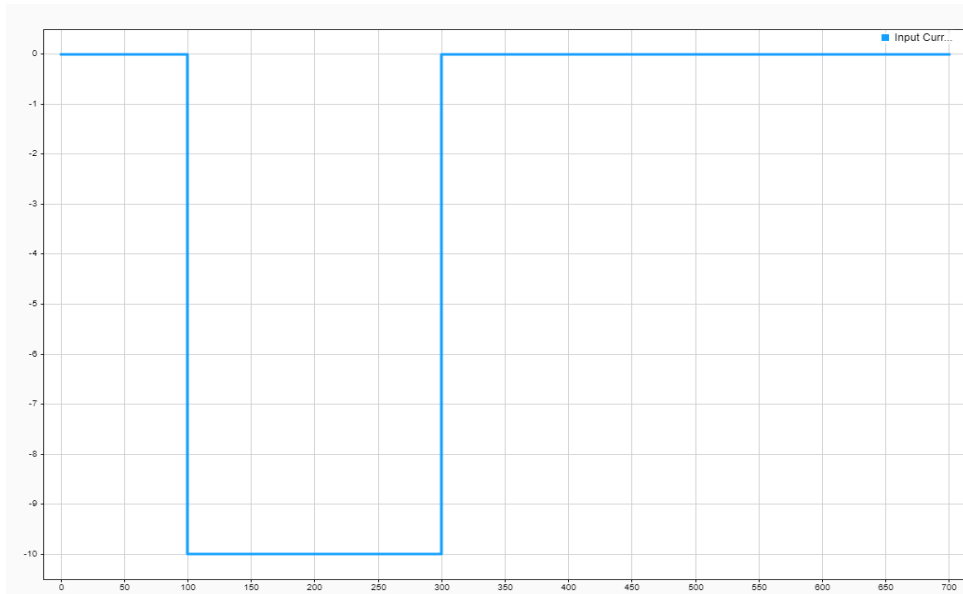


Figure 5.2 Input current pulse.

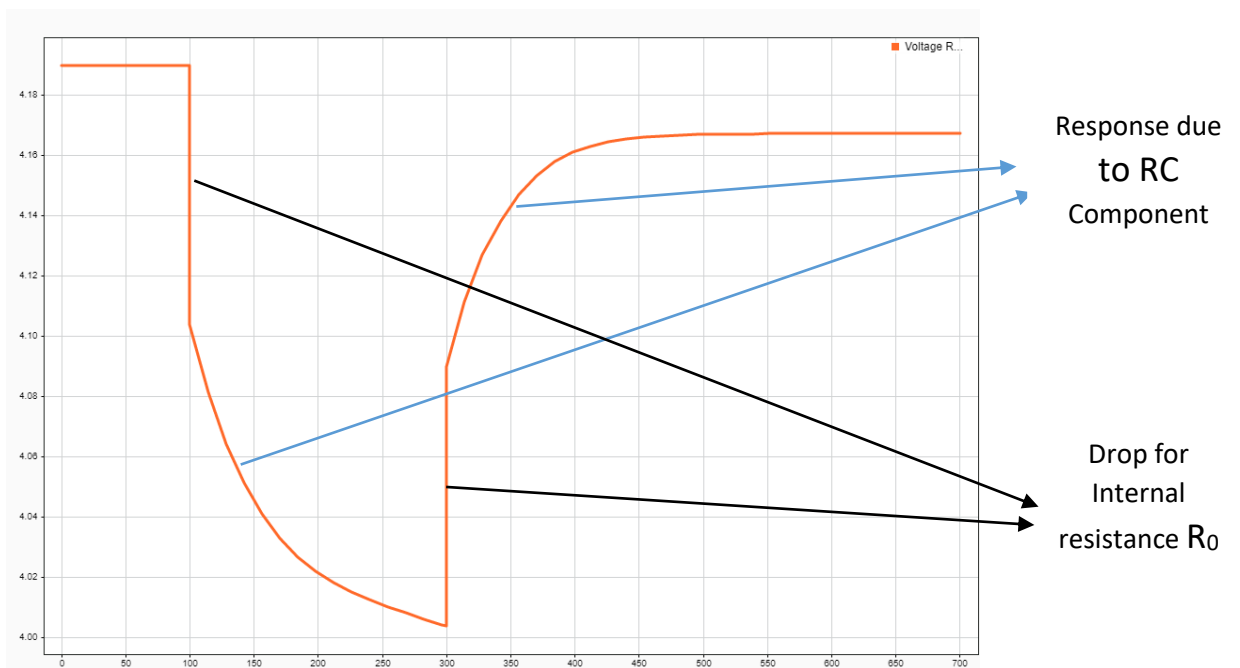


Figure 5.3 Output voltage characteristics

The ECM (Electrical Circuit Model) of battery is a simple model and it is easy to implement and also captures the dynamic very well. The internal resistance with 1RC or 2 RC payer is sufficient to describe the output dynamically.

5.3.2 1RC Battery Model

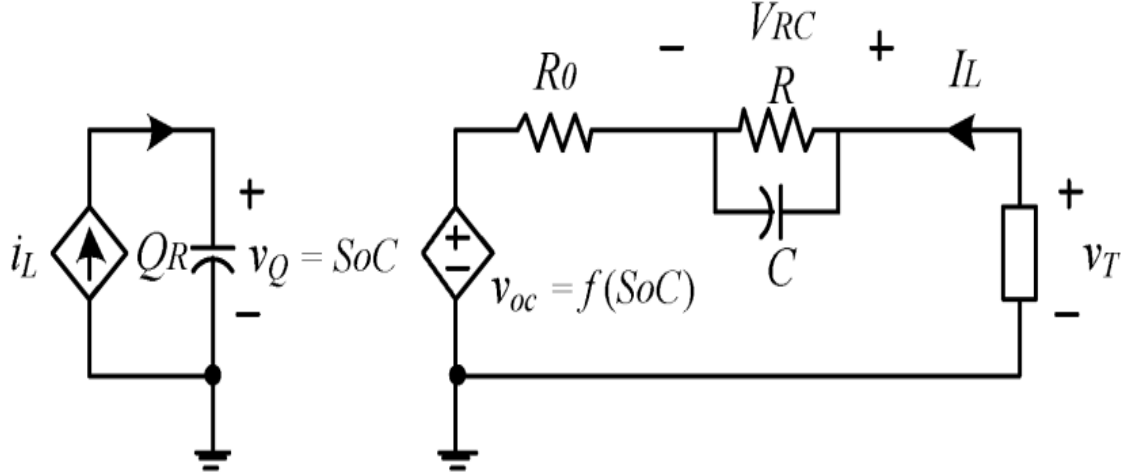


Figure 5.4 1RC Battery Model [20]

Battery model internal resistance with RC parallel component is the best model. In this model figure 5.4 R_0 is internal resistance that, from an electrochemical standpoint, describes the electrolyte resistance. Additionally, it explains the ohmic decrease or rise that occurs when the battery is utilized or stopped. R_1 and C_1 describe the diffusion and surface reaction and it follows the ohmic drop and exponential dynamic of the terminal voltage. The mathematical expression of the model.

$$V_{R_1C_1} = R_1(i_L - i_{C_1}) \quad (5.1)$$

$$V_{R_1C_1} = R_1\left(i_L - C_1 \frac{dV_{R_1C_1}}{dt}\right) \quad (5.2)$$

$$\dot{V}_{R_1C_1} = -\frac{V_{R_1C_1}}{R_1C_1} + \frac{1}{C_1}i_L \quad (5.3)$$

The SOC of The Battery at time t when the available capacity of the Battery Q_{av} , and the load current i_L .

$$SOC = \frac{Q_r}{Q_{av}} \quad (5.4)$$

$$SOC(t) = f(i_L, Q_{av}) = SOC(t_0) + \frac{1}{Q_{av}} \int_{t_0}^{t_1} i_L dt \quad (5.5)$$

$$V_T = V_{0c} + V_{R_0} + V_{R_1 C_1} \quad (5.4)$$

$$V_{R_0} = R_0 i_L \quad (5.5)$$

$$V_{0c}(SOC) = a_i SOC + b_i \quad (5.6)$$

Where

a_i is the slope of the SOC- V_{0c} Curve.

b_i is the initial value of OCV.

$$V_T - b_i = a_i SOC + V_{R_0} + V_{R_1 C_1} \quad (5.7)$$

The state space model for this model for SOC Estimation where SOC is one of the States and another State is $V_{R_1 C_1}$ voltage across the RC payer

$$\dot{x} = Ax + Bi_L$$

$$V_T = Cx + Di_L \quad (5.8)$$

The State Matrix A, B, C, and D from above equations 5.1, 5.3 and 5.7.

$$A = \begin{bmatrix} 0 & 0 \\ 0 & -\frac{1}{R_1 C_1} \end{bmatrix} ; \quad B = \begin{bmatrix} \frac{1}{Q_{av}} \\ \frac{1}{c_1} \end{bmatrix}$$

$$C = [a_i \quad 1] ; \quad D = [R_0] . \quad (5.9)$$

5.3.3 High-Fidelity Electrical Model (1RC)

In our previous Battery model, we took V_{oc} (Open circuit voltage) as the function of SOC (State of Charge) and other Parameters like R_0 , R_1 , and C_1 are not a function of SOC or T (temperature). For the accurate run time SOC estimation we should include the variation of the Parameter concerning SOC and temperature [18] that is all parameters of the battery should be the function of SOC and T .

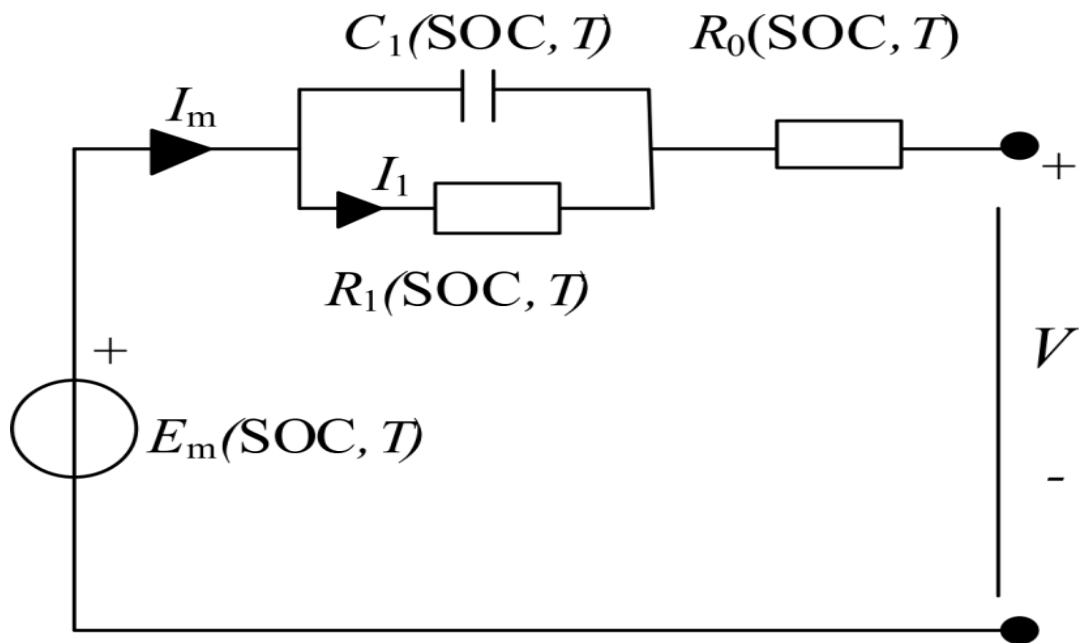


Figure 5.5 ECM with SOC and T dependent [18]

The parameter of the Equivalent Circuit Battery

$$V_{OC} = E_M (SOC, T)$$

$$R_0 = R_0 (SOC, T)$$

$$R_1 = R_1 (SOC, T)$$

$$C_1 = C_1 (SOC, T)$$

Several discharge tests at various temperatures were conducted using the parameter estimate procedure. Each of these four equivalent circuit elements has two-dimensional look-up tables provided by the results obtained.

Every circuit element was a subsystem made up of blocks for computing the element's attributes as well as specially designed electrical blocks. Create the Thevinin equivalent model with that block.

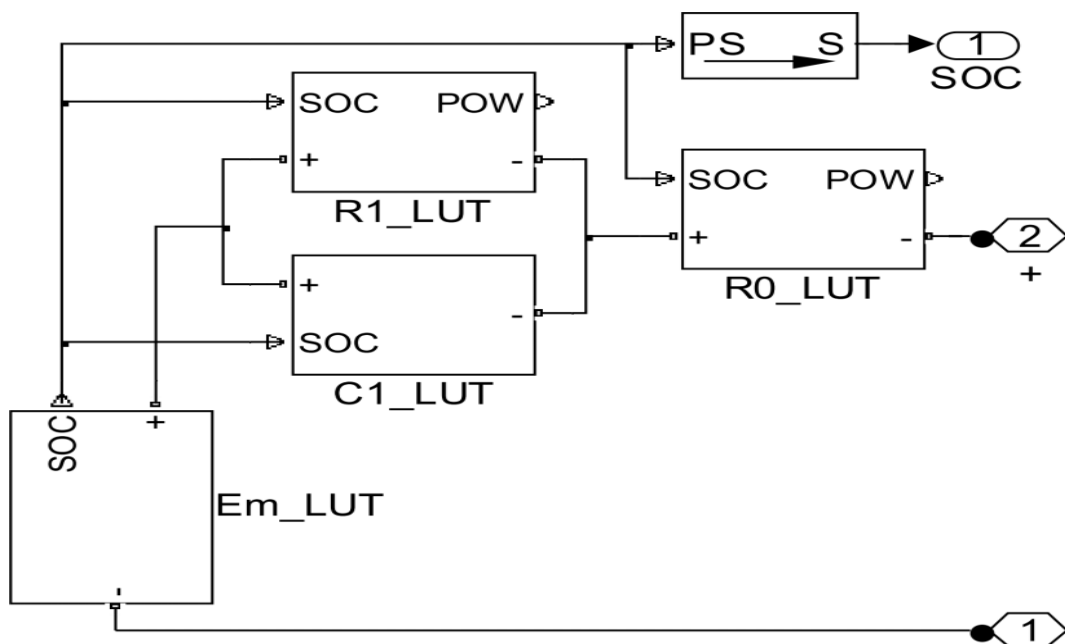


Figure 5.6 Battery Simscape block model [18]

Look-up tables were chosen for the parameterization of the circuit element. Every circuit element's lookup tables were selected using seven distinct SOC points, with SOC breakpoints distributed with a bias slightly toward low and high SOC.

The previous experiment here also did the same thing first tested a 31 Ah Battery in the lab by the discharge current pulse and collected the output voltage data, using the Control System Optimization Toolbox from MATLAB Toolbox and Lounge Parameter Optimization After some iteration the parameters E_M , R_0 , R_1 , and C_1 produce 2D look-up table value.

5.3.4 2RC Battery Model

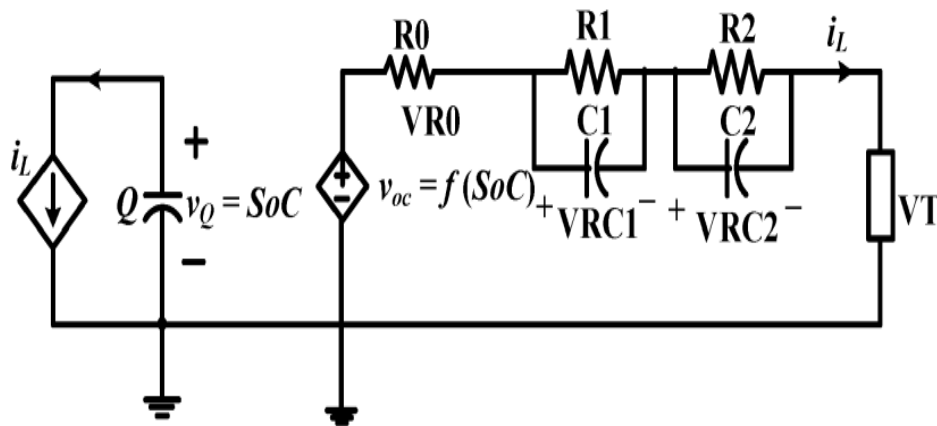


Figure 5.7 2RC Battery Model [2]

Battery model internal resistance with RC parallel component is the best model. The ECM model with 1RC is a good model but the 2RC

model is a more accurate model to represent the battery dynamic two times constant which helps properly capture the transient response. The model figure 5.13 R_0 is internal resistance that, from an electrochemical standpoint, describes the electrolyte resistance. Additionally, it explains the ohmic decrease or rise that occurs when the battery is utilized or stopped. R_1 , C_1 , and R_2 , C_2 describe the diffusion and surface reaction and it follows the Ohmic drop and exponential dynamic of the terminal voltage.

The mathematical expression of the model.

$$SOC(t) = f(i_L, Q_{av}) = SOC(t_0) + \frac{1}{Q_{av}} \int_{t_0}^{t_1} i_L dt \quad (5.10)$$

$$\dot{V}_{RC1} = -\frac{V_{RC1}}{R_1 C_1} + \frac{1}{C_1} i_L \quad (5.11)$$

$$\dot{V}_{RC2} = -\frac{V_{RC2}}{R_2 C_2} + \frac{1}{C_2} i_L \quad (5.12)$$

$$V_{R_0} = R_0 i_L \quad (5.13)$$

The output voltage equation

$$V_T = V_{R_0} + V_{RC1} + V_{RC2} \quad (5.14)$$

The state space model of the 2RC model

$$\begin{aligned} \dot{x} &= Ax + Bi_L \\ V_T &= Cx + Di_L \end{aligned} \quad (5.15)$$

The states are SOC, the voltage across the first RC component

V_{RC1} , and the voltage across the second RC payer V_{RC2}

$$x = \begin{bmatrix} SOC \\ V_{RC1} \\ V_{RC2} \end{bmatrix} \quad (5.16)$$

The A, B, C, and D matrixes are

$$A = \begin{bmatrix} 0 & 0 & 0 \\ 0 & -\frac{1}{RC1} & 0 \\ 0 & 0 & -\frac{1}{RC2} \end{bmatrix}; \quad B = \begin{bmatrix} \frac{1}{Qr} \\ \frac{1}{C1} \\ \frac{1}{C2} \end{bmatrix};$$

$$C = [ai \quad 1 \quad 1]; \quad D = [R_0]; \quad (5.17)$$

Where ai is the slope of the V_{OC} -SOC curve and Qr is the available capacity of the Battery.

5.4 Observability Check of the State Space Model

The conventional State-Space model of the Battery

$$\begin{aligned} \dot{x} &= Ax + Bi_L \\ V_T &= Cx + Di_L \end{aligned} \quad (5.10)$$

State of the model $X = \begin{bmatrix} SOC \\ V_{oc} \end{bmatrix};$

$$\begin{aligned}
A &= \begin{bmatrix} 0 & 0 \\ 0 & -\frac{1}{R_1 C_1} \end{bmatrix} \quad ; \quad B = \begin{bmatrix} \frac{1}{Q_{av}} \\ \frac{1}{c_1} \end{bmatrix} \\
C &= [a_i \quad 1] \quad ; \quad D = [R_0] \quad (5.11)
\end{aligned}$$

The observability matrix of the model is

$$O = \begin{bmatrix} C \\ CA \end{bmatrix} = \begin{bmatrix} a_i & 1 \\ 0 & -\frac{1}{R_1 C_1} \end{bmatrix} \quad (5.12)$$

The Observability matrix is a function of a_i which is the slope of the V_{OC} –SOC curve. The observability matrix is full rank when the a_i is nonzero. The value of $|a_i|$ in the range of 30% to 45% is very small shown in Figure 5.14.

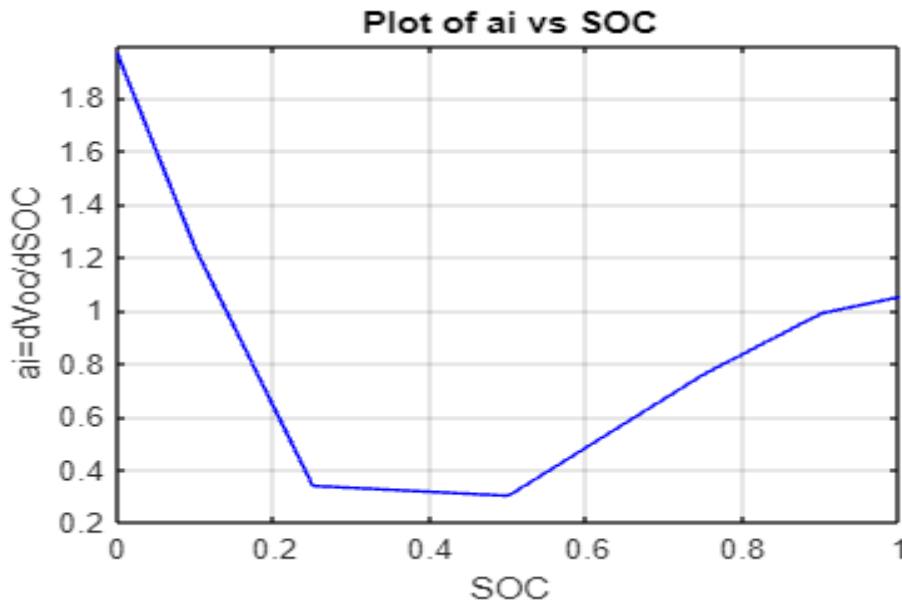


Figure 5.8 Plot of a_i vs SOC

The Steady-State SOC estimation error is sensitive to the slope of the VOC–SOC curve [20] and the error is larger when the SOC range is 30% to 45%.

5.4.1 Proposed New State Space Model

The proposed new state-space space for the model is the open-circuit voltage V_{oc} and the voltage across the RC payer $V_{R_1C_1}$ [20]. The SOC of the battery can be estimated based on the estimated open circuit voltage.

State 1) Open circuit voltage

2) Voltage across the RC payer

$$Z = \begin{bmatrix} V_{oc} \\ V_{R_1C_1} \end{bmatrix} \quad (5.13)$$

$$\dot{z} = Az + Bi_L$$

$$V_T = Cz + Di_L \quad (5.14)$$

Where i_L is the load current and V_T is the terminal voltage. The model matrices A, B, C, and D are.

$$A = \begin{bmatrix} 0 & 0 \\ 0 & -\frac{1}{R_1C_1} \end{bmatrix} ; \quad B = \begin{bmatrix} \frac{a_i}{Q_{av}} \\ \frac{1}{c_1} \end{bmatrix}$$

$$C = [1 \ 1] \quad ; \quad D = [R_0] ; \quad (5.15)$$

The observability matrix of this model

$$O = \begin{bmatrix} C \\ CA \end{bmatrix} = \begin{bmatrix} 1 & 1 \\ 0 & -\frac{1}{R_1 C_1} \end{bmatrix} \quad (5.16)$$

Equation (5.16) represents the observability matrix of the suggested state-space model. The observability matrix is independent of a_i and is always complete rank. The battery state-space model's full rank observability matrix shows that every state is observable across the whole SOC range. After choosing V_{OC} as one of the states in the state-space model, the observability matrix derivation demonstrates that the suggested state-space model is well-conditioned over the whole SOC range. This approach's drawback is that the SOC- V_{OC} profile's slope cannot equal zero, which prevents the SOC from being calculated from the predicted V_{OC} .

5.5 Battery Parameter Identification

The Parameter of the Battery model needs to be estimated. Battery parameter identification refers to the process of determining and characterizing various parameters associated with a battery. These

parameters are crucial for understanding the performance, health, and behavior of a battery in different applications. The battery parameter identification process involves a combination of laboratory testing, modeling, and data analysis.

First, we take a 4.2 V lithium-ion Battery test with a current pulse and record the output voltage.

The input current pulse of -10 A duration of 40000 Sec. Record Output Voltage Characteristics

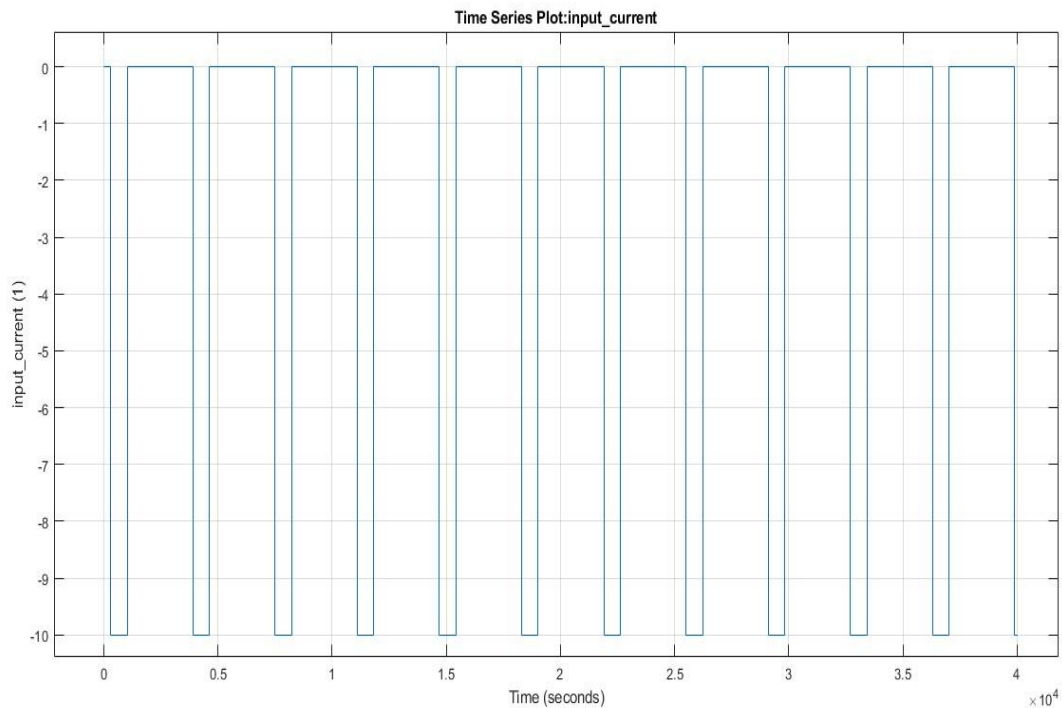


Figure 5.9 Input current pulse

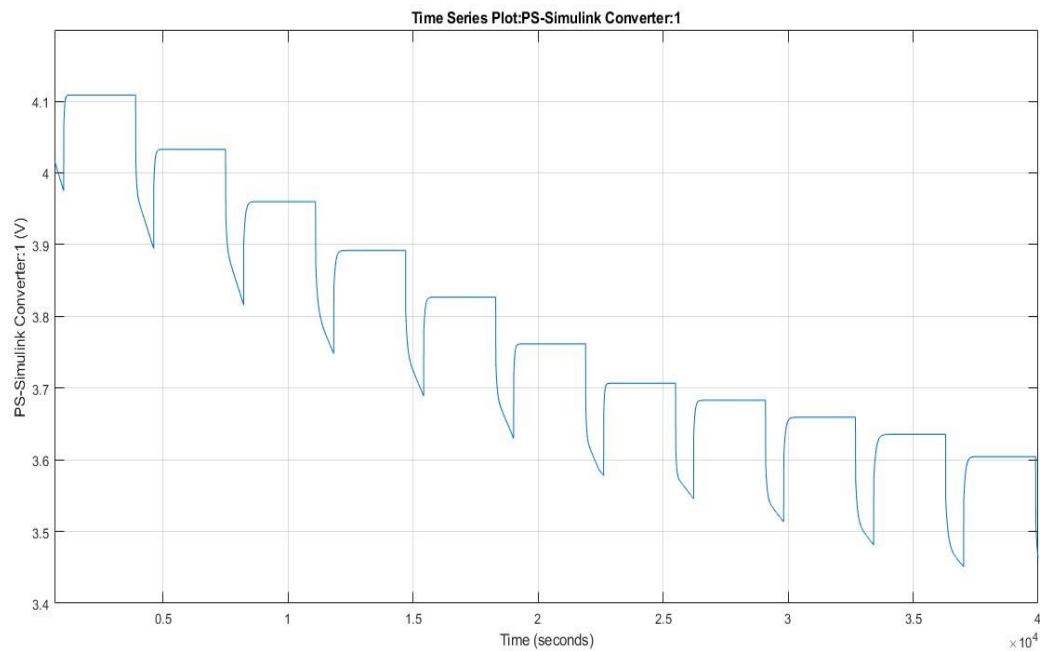


Figure 5.10 Output Voltage from Testing

After recording the Current and Voltage Response create an ECM model of the battery in MATLAB Simscape.

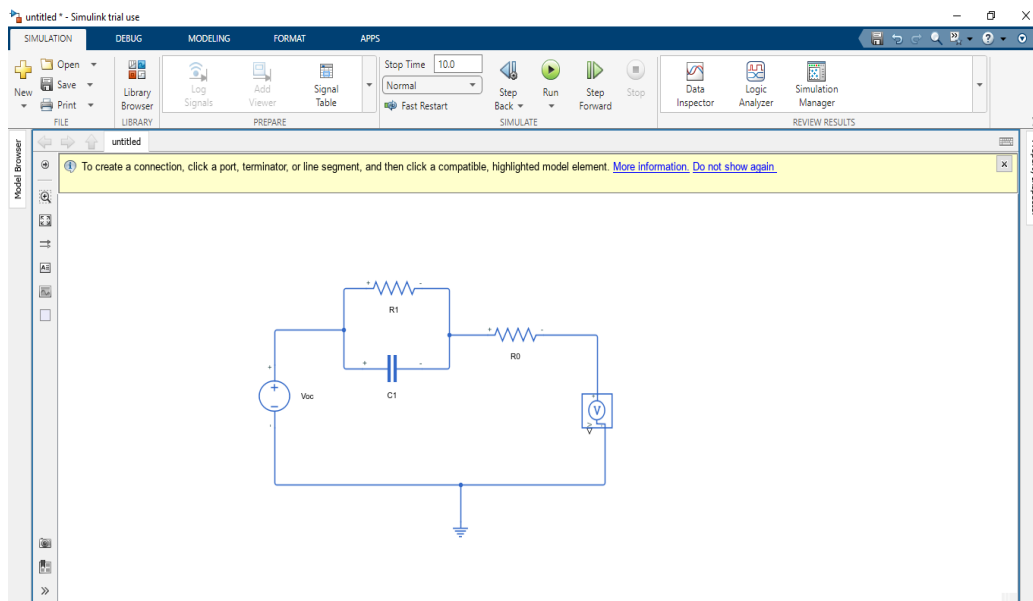


Figure 5.11 ECM model in Simulink

Applied the same current as input and observed the Response Voltage For the initial gauge value of The Parameter. We can observe that there is a huge difference between the Mesernment value and The Simulatate value.

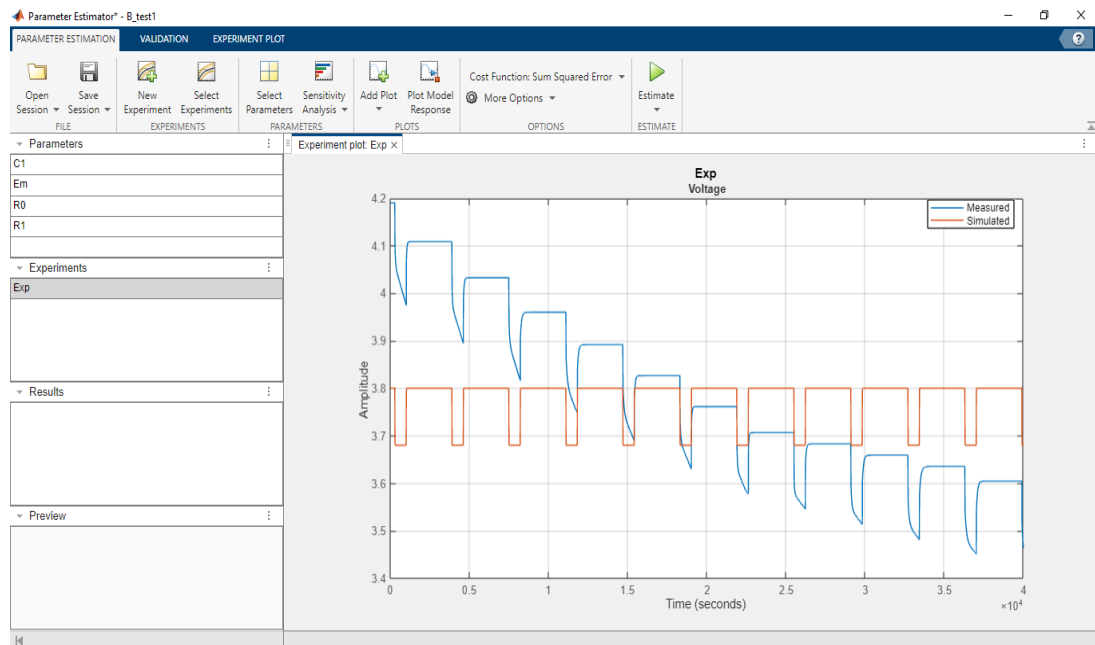


Figure 5.12 Measurement and The Simulated value of voltage

So we use the Control System Optimization Toolbox from MATLAB Toolbox and Lounge Parameter Estimation After some iteration output simulated voltage gradually converges to the Measurement voltage, and the parameters E_M , R_0 , R_1 , and C_1 estimate their actual value.

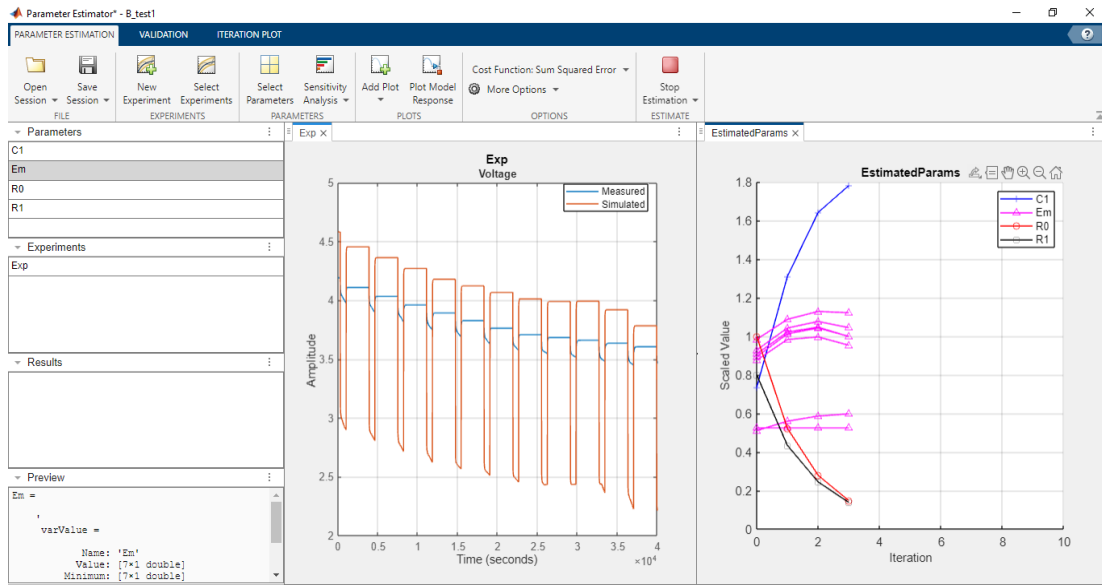


Figure 5.13 Parameter estimation progress

After completing the 12 iterations we can observe that the simulated value and the measurement value almost converse.

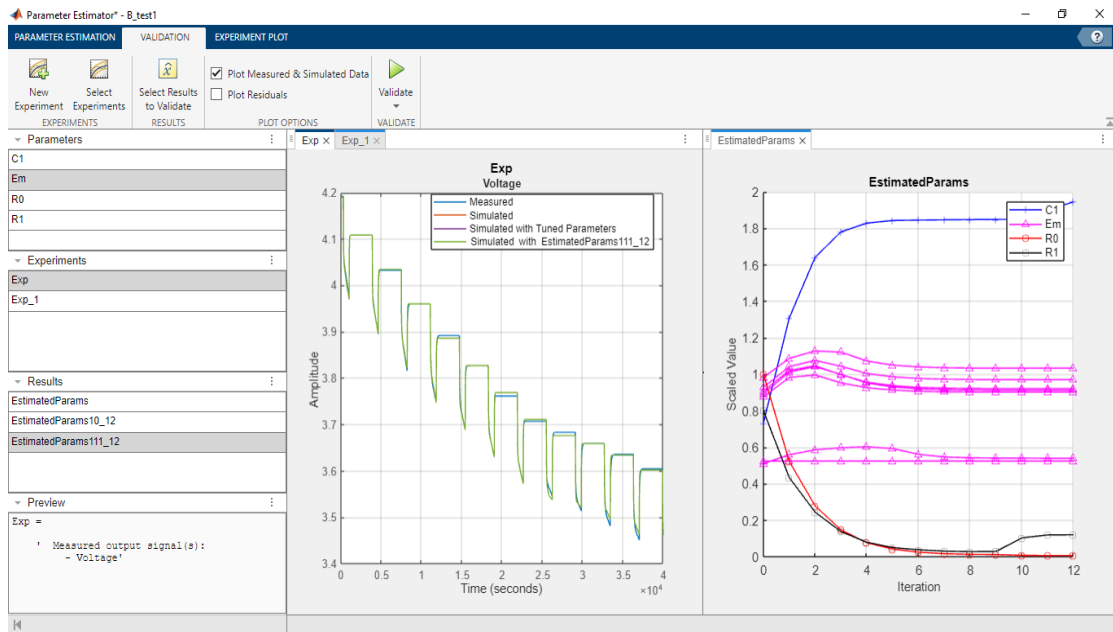


Figure 5.14 Parameter estimation after 12 iteration

Now we have found the proper Battery model with almost accurate parameter values.

Chapter 6

SOC Estimation Using the Unscented Kalman Filter

6.1 Introduction

SOC estimation is a crucial task in battery management systems, particularly for electric vehicles and portable electronics. A technique that is becoming popular in many nonlinear estimating and machine learning applications is the Extended Kalman Filter (EKF). These include the estimation of a nonlinear dynamic system's state, the estimation of parameters for the identification of nonlinear systems, and dual estimation, which involves the simultaneous estimation of states and parameters. The Unscented Kalman Filter (UKF) is an improvement of EKF. The Unscented Kalman Filter (UKF) is a powerful tool for SOC estimation because it can handle nonlinear system models and non-Gaussian uncertainties, which are common in battery systems.

6.2 The Unscented Kalman Filter Algorithm

The UKF algorithm is a filtering algorithm for non-linear systems, distinct from the EKF method because the system equations do not require to be linearized, the system equation is more precise. The dynamic system's state-space equations and measurement equations.

[21]. The algorithm first generates a set of state values called sigma points. These sigma points capture the mean and covariance of the state estimates.

The state transition and measurement equations for an M-state discrete-time nonlinear system have additive process and measurement noise terms with zero mean and covariance Q and R, respectively:

$$x[k + 1] = f(x[k], u_s[k] + w[k] \quad (6.1)$$

$$y[k] = h(x[k], u_m[k] + v[k] \quad (6.2)$$

$$w[k] \sim (0, Q[k])$$

$$v[k] \sim (0, R[k])$$

Initially provide Q as process noise and R as measurement noise.

1) Determine the initial value $x[0]$ of the state variable and the initial covariance matrix p.

$$\hat{x}[0|-1] = E(x[0]) \quad (6.3)$$

$$P[0|-1] = E(x[0] - \hat{x}[0|-1])(x[0] - \hat{x}[0|-1])^T \quad (6.4)$$

Here

\hat{x} is the state estimate and $\hat{x} [k_a | k_b]$ denotes the state estimate at time step k_a using measurements at time steps 0,1,..., k_b . So $\hat{x} [0|-1]$ is

the best guess of the state value before you make any measurements. You specify this value when you construct the filter.

2) For each time step k , update the state and state estimation error covariance using the measured data, $y[k]$. In the software, the correct command performs this update.

i) Choose the sigma points $\hat{x}^{(i)}[k | k - 1]$ at time step k .

$$\hat{x}^{(0)}[k | k - 1] = x[k | k - 1] \quad (6.5)$$

$$\hat{x}^{(i)}[k | k - 1] = x[k | k - 1] + \Delta x^{(i)} \quad i = 1, \dots, 2M \quad (6.6)$$

$$\Delta x^{(i)} = (\sqrt{c^P[k | k - 1]})^T i \quad i = 1, \dots, M \quad (6.7)$$

$$\Delta x^{(M+i)} = -(\sqrt{c^P[k | k - 1]})^T i \quad i = 1, \dots, M \quad (6.8)$$

Where

$c = \alpha^2(M + k)$ is a scaling factor.

\sqrt{cP} is the Matrix square root of cP

ii) Use the nonlinear measurement function to compute the predicted measurements for each of the sigma points.

$$\hat{y}^{(i)}[k | k - 1] = h(\hat{x}^{(i)}[k | k - 1], u_m[k]) \quad i = 0, 1, \dots, 2M \quad (6.9)$$

iii) Combine the predicted measurements to obtain the predicted measurement at time k.

$$\hat{y}[k] = \sum_{i=0}^{2M} W_M^{(i)} \hat{y}^{(i)}[k|k-1] \quad (6.10)$$

$$W_M^{(0)} = 1 - \frac{M}{\alpha^2(M+k)} \quad (6.11)$$

$$W_M^i = \frac{M}{2\alpha^2(M+k)} \quad i = 1, 2, \dots, 2M \quad (6.12)$$

iv) Estimate the covariance of the predicted measurement. Add $R[k]$ to account for the additive measurement noise.

$$p_y = \sum_{i=0}^{2M} W_c^{(i)} \hat{y}^{(i)}[k|k-1] - \hat{y}[k] (\hat{y}^{(i)}[k|k-1] - \hat{y}[k])^T + R[k] \quad (6.13)$$

$$w_c^{(0)} = (2 + \alpha^2 + \beta) - \frac{M}{\alpha^2(M+k)} \quad (6.14)$$

$$w_c^i = \frac{1}{2\alpha^2(M+k)} \quad i = 1, 2, \dots, 2M \quad (6.15)$$

v) Estimate the cross-covariance between $\hat{x}[k|k-1]$ and $\hat{x}[k]$

$$P_{xy} = \frac{M}{2\alpha^2(M+k)} \sum_{i=0}^{2M} (\hat{x}^{(i)}[k|k-1] - \hat{x}[k|k-1]) (\hat{y}^{(i)}[k|k-1] - \hat{y}[k]^T) \quad (6.16)$$

The summation starts from $i = 1$ because

$$\hat{x}^{(0)}[k|k-1] - \hat{x}[k|k-1] = 0 \quad (6.17)$$

vi) Obtain the estimated state and state estimation error covariance at time step k.

$$K = P_{xy}P_y^{-1} \quad (6.18)$$

$$\hat{x}[k|k] = \hat{x}[k|k-1] + K(y[k] - \hat{y}[k]) \quad (6.19)$$

$$P[k|k] = P[k|k-1] - KP_yK_k^T \quad (6.20)$$

Where K is the Kalman gain.

3) Predict the state and state estimation error covariance at the next time step.

i) Choose the sigma points $\hat{x}^{(i)}[k|k]$ at time step k.

$$\hat{x}^{(0)}[k|k] = \hat{x}[k|k] \quad (6.21)$$

$$\hat{x}^{(i)}[k|k] = \hat{x}[k|k] + \Delta x^{(i)} \quad i = 1, 2, \dots, 2M \quad (6.22)$$

$$\Delta x^{(i)} = (\sqrt{cP[k|k]})i \quad i = 1, \dots, M \quad (6.23)$$

$$\Delta x^{(M+i)} = -(\sqrt{cP[k|k]})i \quad i = 1, \dots, M \quad (6.24)$$

ii) Use the nonlinear state transition function to compute the predicted states for each of the sigma points.

$$\hat{x}^{(i)}[k+1|k] = f(\hat{x}^{(i)}[k|k], u_s[k]) \quad (6.25)$$

iii) Combine the predicted states to obtain the predicted states at time k+1.

$$\hat{x}[k+1|k] = \sum_{i=0}^{2M} W_M^{(i)} \hat{x}^{(i)}[k+1|k] \quad (6.26)$$

$$W_M^{(0)} = 1 - \frac{M}{\alpha^2(M+k)} \quad (6.27)$$

$$W_M^i = \frac{M}{2\alpha^2(M+k)} \quad i = 1, 2, \dots, 2M \quad (6.28)$$

iv) Compute the covariance of the predicted state. Add $Q[k]$ to account for the additive process noise

$$P[k+1|k] = \sum_{i=0}^{2M} W_c^{(i)} (\hat{x}^{(i)}[k+1|k] - \hat{x}[k+1|k]) (\hat{x}^{(i)}[k+1|k] - \hat{x}[k+1|k])^T + Q[k] \quad (6.29)$$

$$W_c^{(0)} = (2 - \alpha^2 + \beta) - \frac{M}{\alpha^2(M+k)} \quad (6.30)$$

$$W_c^i = \frac{1}{2\alpha^2(M+k)} \quad i = 1, 2, \dots, 2M \quad (6.31)$$

The previous algorithm is implemented assuming additive noise terms in the state transition and measurement equations [22].

6.3 SOC estimation of the derived model

In MATLAB using physical modeling interfaces, Simscape makes the battery an Electrical Equivalent circuit model (2RC). Thermal modeling for proper estimation. using Simcape language create the battery, resistance, and capacitor the signal builder that generates the input signal, the current is the same as the discharge current used in the experiment.

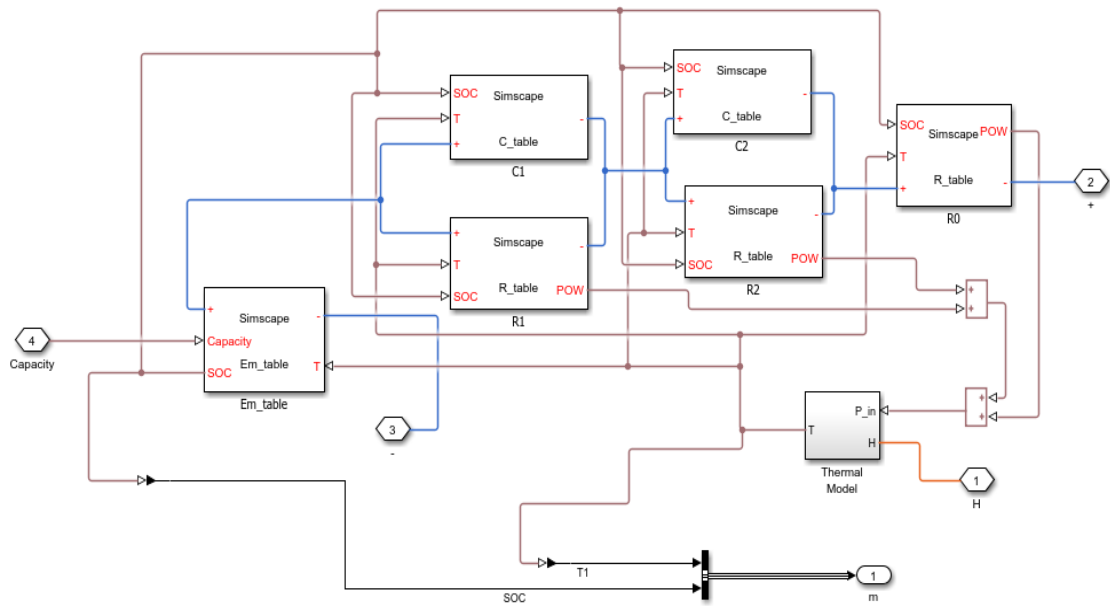


Figure 6.1 Electrical Equivalent Circuit Model (2RC)

Use the unscented Kalman filter for the SOC estimation. first, write the state equation in Simscape with the help of the MATLAB function. Using a 2D look-up table to represent the parameter value that gets from parameter estimation.

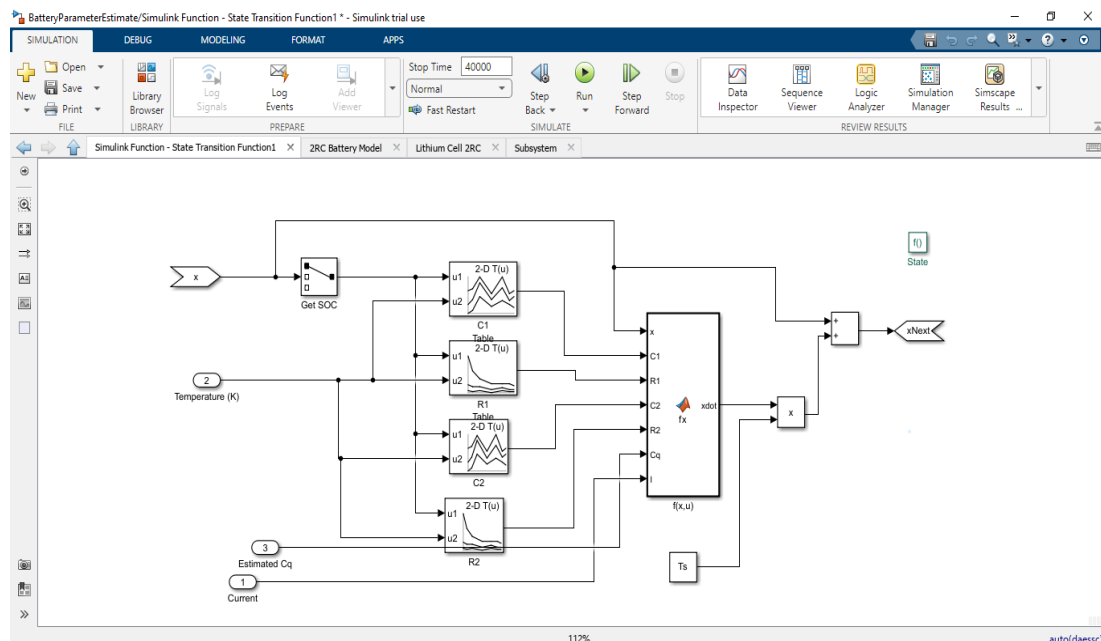


Figure 6.2 State transition equation block

Now the Measurement equation is written using the MATLAB function block

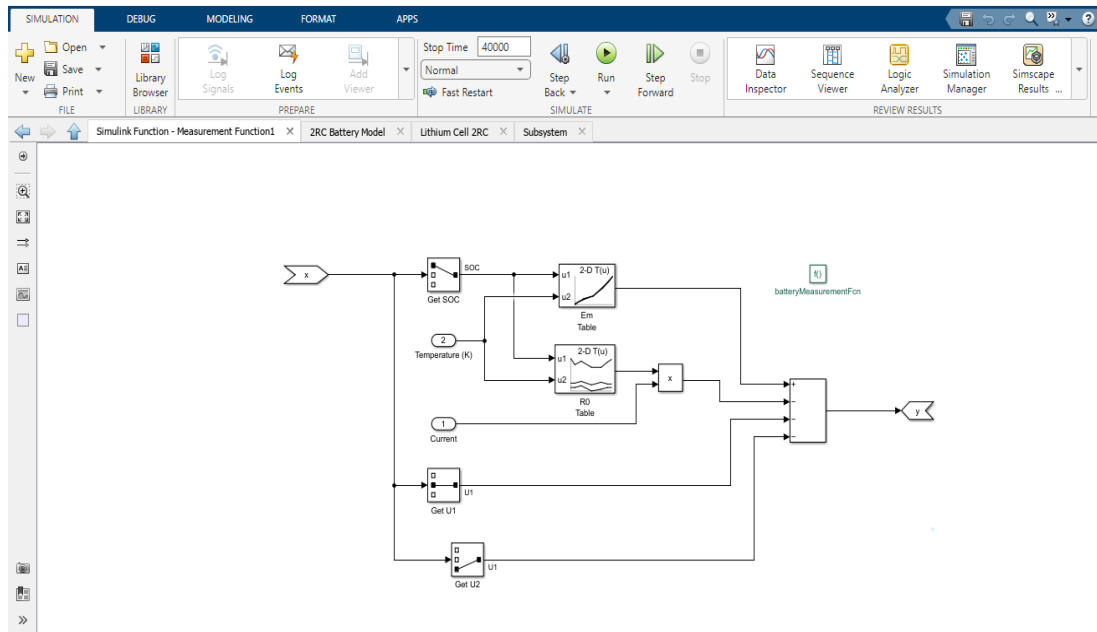


Figure 6.3 Measurement equation block

Creating battery model, state transition equation, and measurement equation in the MATLAB Simulink environment using all that create a block diagram for SOC estimation. Use an Unscented Kalman filter block for Battery State of Charge estimation.

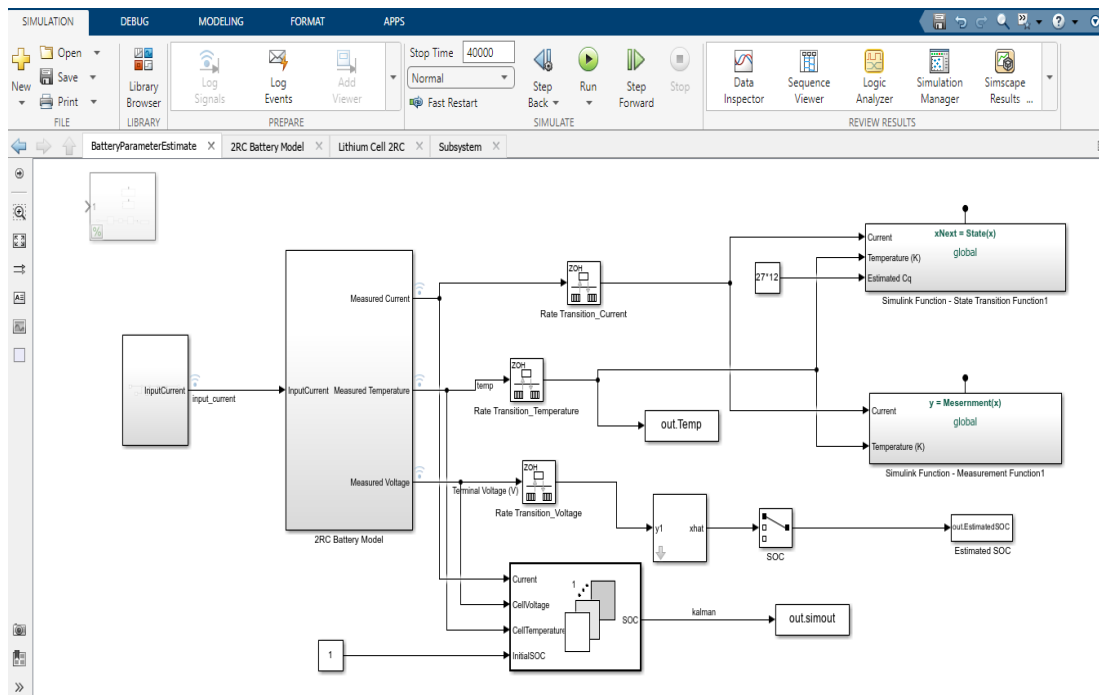


Figure 6.4 Simulink block of SOC estimation

Create this model and write MATLAB code to run the program and simulation to get the SOC estimated result. There are several subsystems in the Simulink block: input current block, 2RC battery model block, state transition block, measurement block, and unscented Kalman filter block.

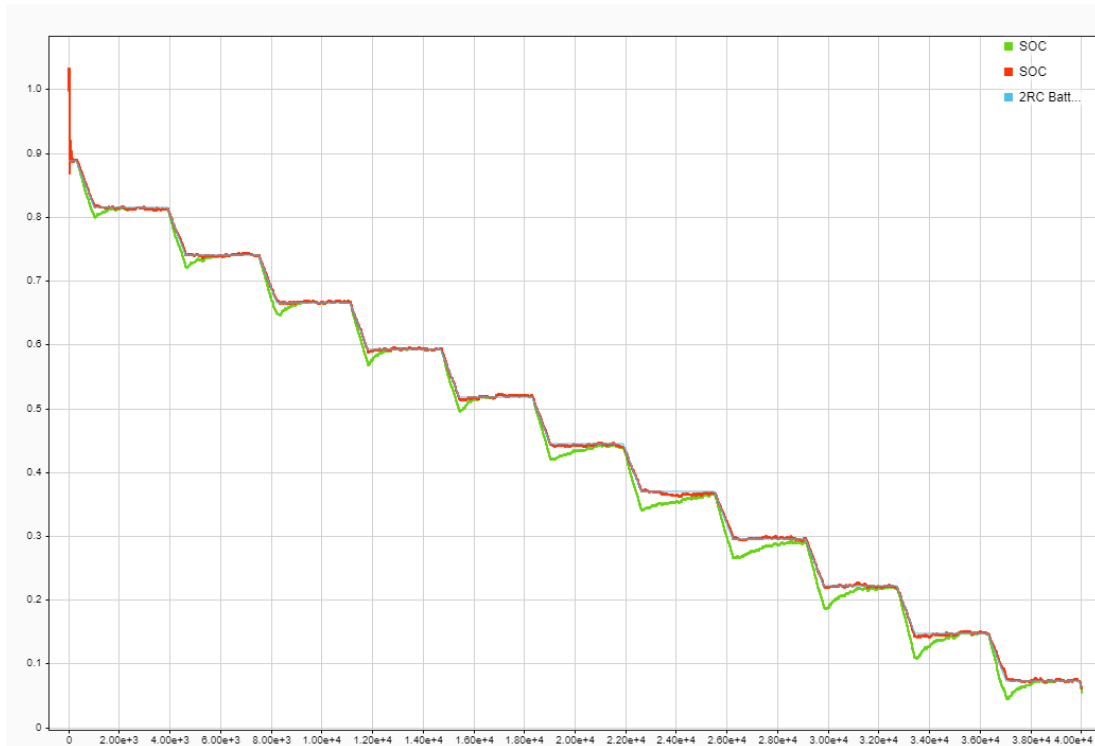


Figure 6.5 SOC simulation data

In the simulation result sky blue line represents the Real SOC of the battery, the Green represents the conventional state-space output and the Red line is the estimated SOC of the 2RC equivalent circuit new state-space model of a lithium-ion battery.

Chapter 7

Discussion and Conclusion

7.1 Comparative Study of Simulation

This thesis uses two different state space models. One is the conventional method where the state of the model is the SOC, and the voltage across the RC component v_{RC} is the other state.

The new State-Space model where Open circuit voltage V_{oc} is one of the states and Voltage across the RC component v_{RC} is another state

The input current and the voltage response of both model

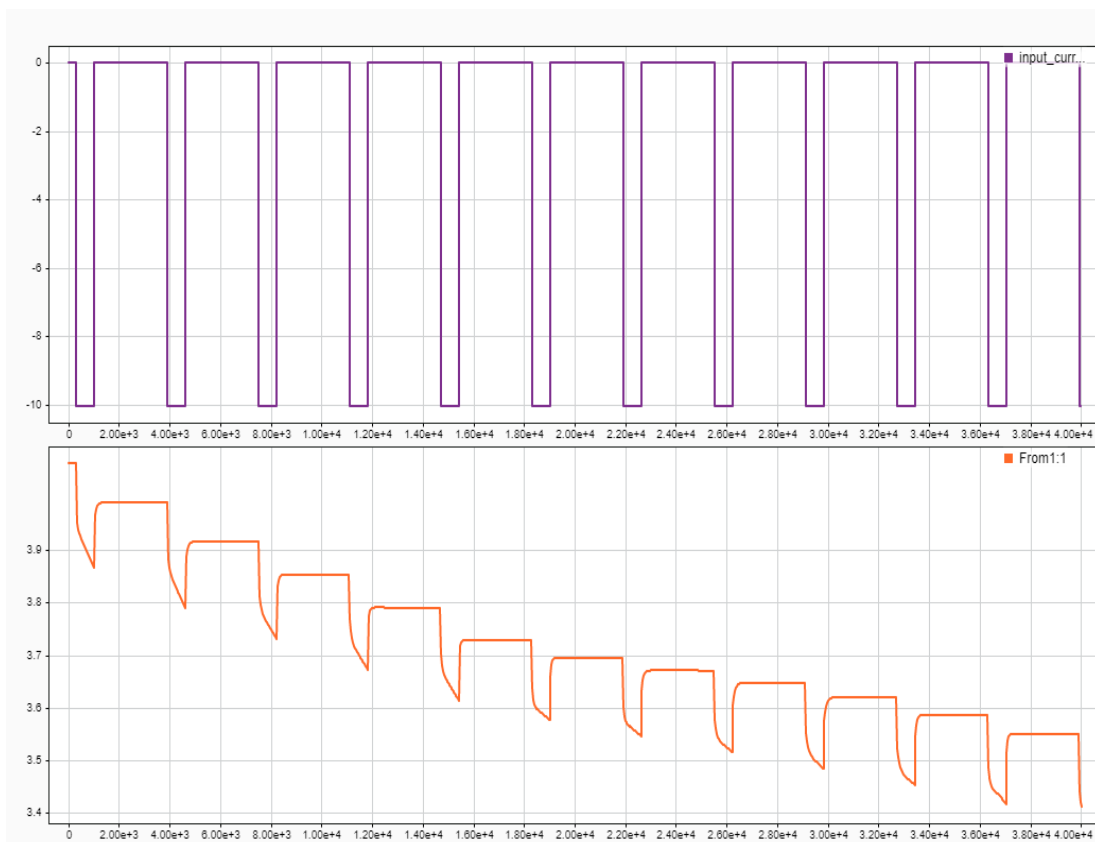


Figure 7.1 current and voltage profile for Experiment

Use experimental temperature 293K or 20°C and the temperature graph in the whole experiment is

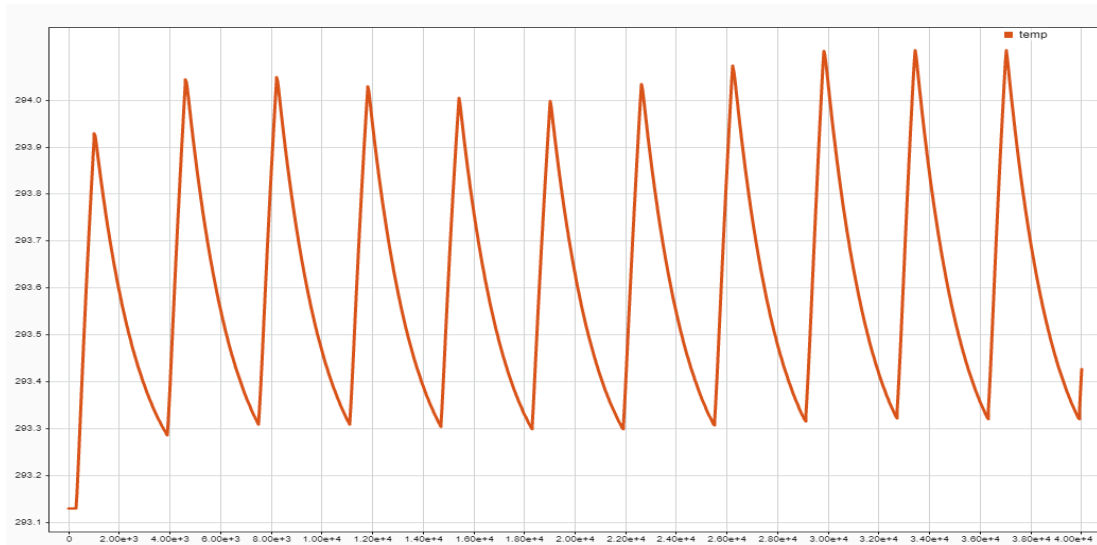


Figure 7.2 Temperature response plot

For the conventional state space, the SOC response and error.

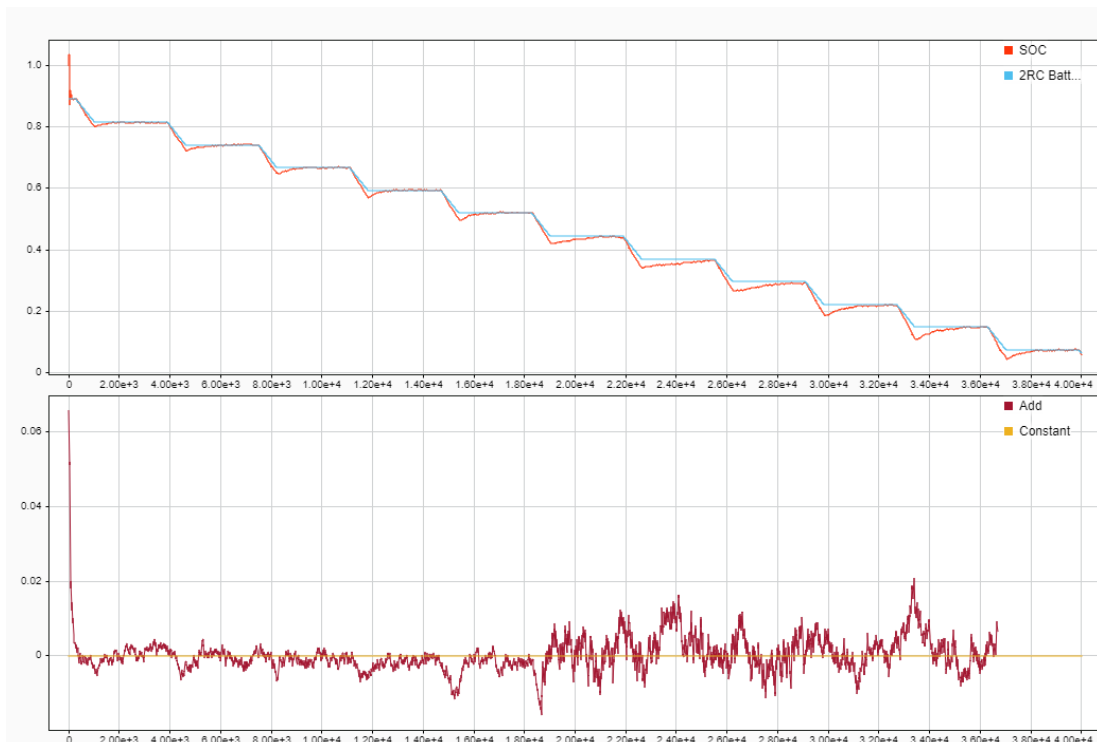


Figure 7.3 SOC Response and Estimation Error plot

When the SOC is low between 45% to 25%, less than 50% then The SOC estimation error is comparatively more. So resolving that problem creates.

A new state-space model where The State of the model is different

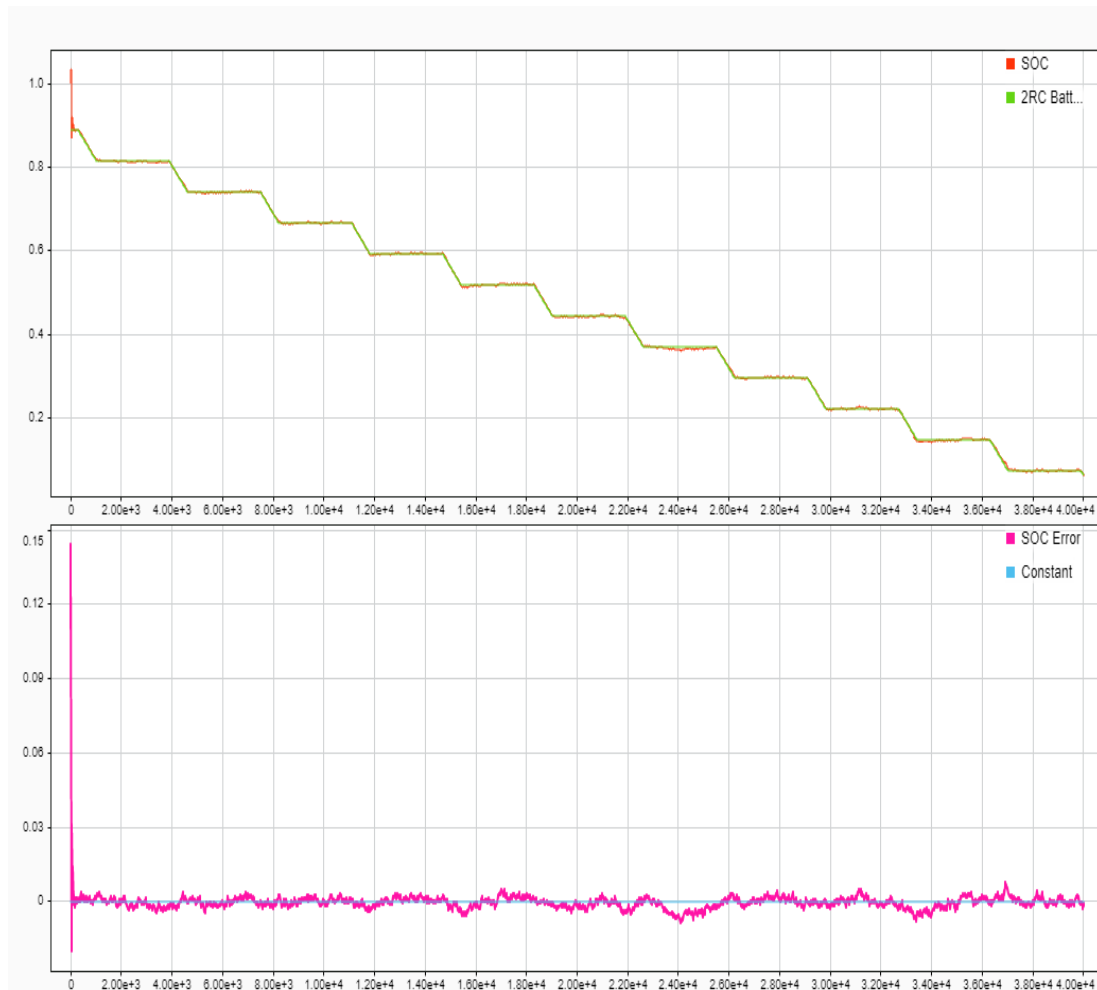


Figure 7.4 SOC Error and the response of the new model

The new state space model produces a better estimation compared to the conventional method.

All the responses are shown in Figure 7.5 and the comparative error is shown in Figure 7.6.

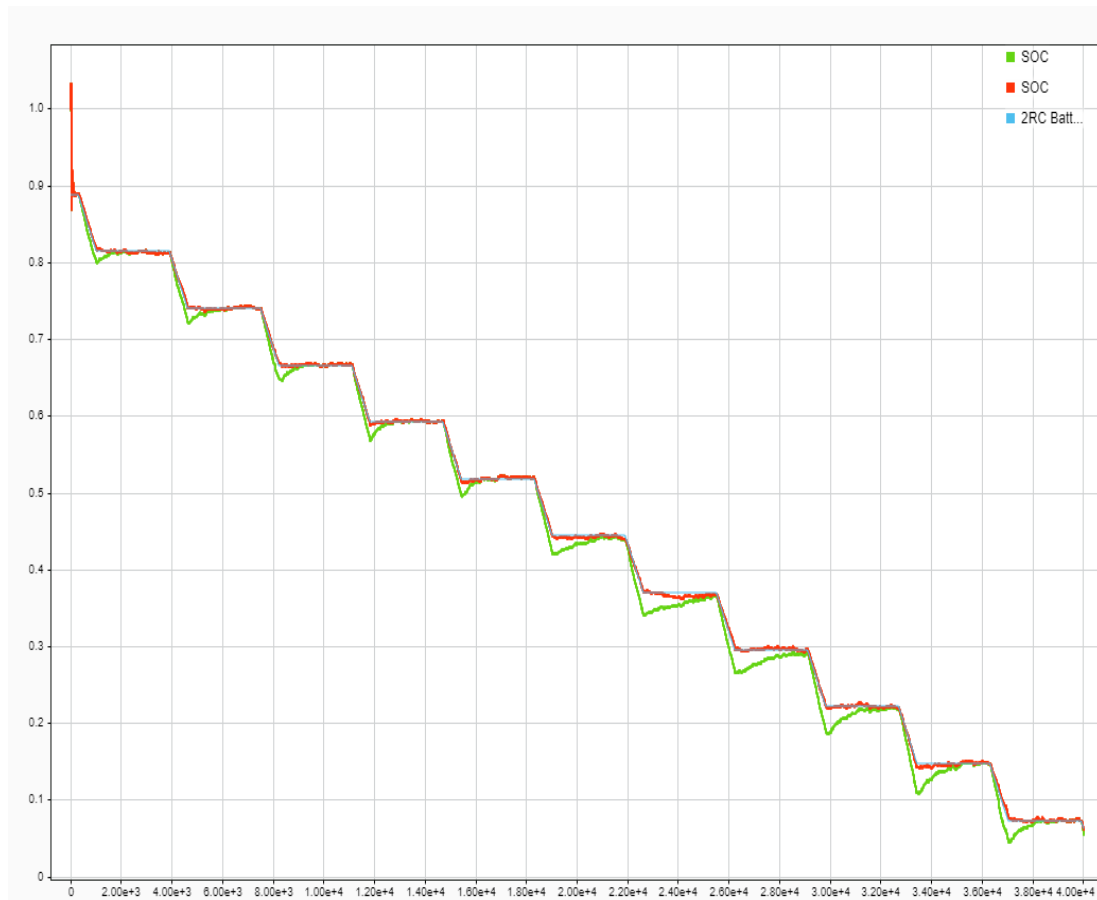


Figure 7.5 SOC response of conventional and new model

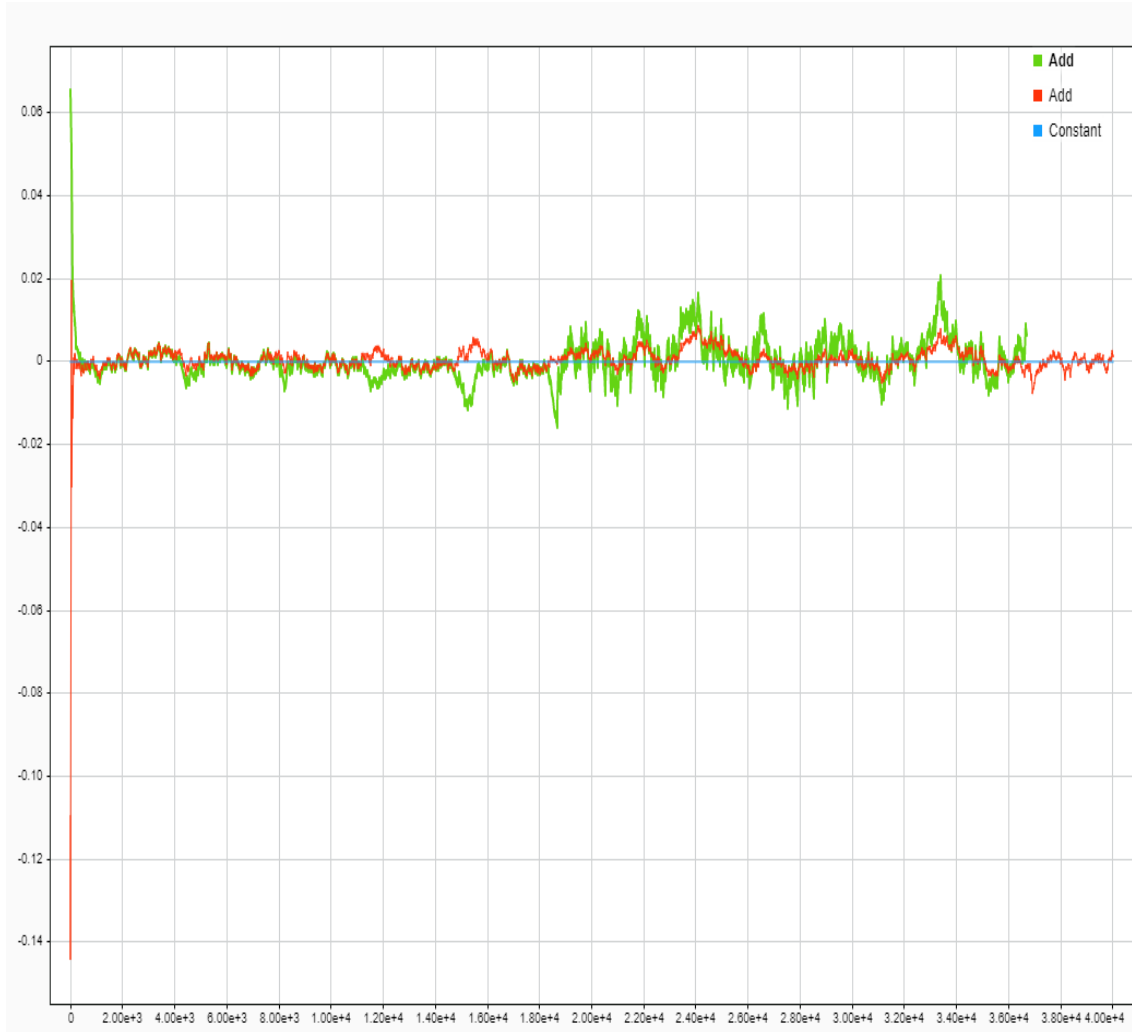


Figure 7.6 Error in SOC Estimation of different method

7.2 Discussion

In this thesis work we estimate SOC of lithium-ion battery in two different state space model using the Unscented kalman filter. When we use conventional state space model SOC of the battery is a state to observe for SOC estimation and we fiend that more error in 30% to 45% of SOC of battery irrespective of observer at the estimation result shows in the figure 7.3 and 7.6 (green colour plot is the response figure 7.6 of conventional method). Now when change the state space of the

model and take new State Open Circuit Voltage in the place of SOC, a significant change noticed in the that range (30%-45%). In figure 7.4 and 7.6(Red simulation plot in 7.6). the simulation result shown in figure 7.5 and 7.6 describe the improvement of result and this is very close to the real SOC of battery.

7.3 Conclusion and Future work

This chapter analyses the response of the different models. Conventional state space SOC and Voltage across RC component and new state space selected where SOC is replaced with Open Circuit voltage (VOC) and investigate by High Fidelity Electrical model of lithium ion battery using Unscented Kalman Filter (UKF) algorithm and get a good improvement in SOC estimation result and solve the observability issue of conventional state space method.

In future the building of BMS, when a large number of cell use in the BMS this model helps to reduce the SOC estimation error. Using this method make more efficient BMS for EV, HEV and small and micro power grid application.

REFERENCES

- [1] H. Rahimi-Eichi, F. Baronti, and M.-Y. Chow, “Online adaptive parameter identification and state-of-charge co-estimation for lithium polymer battery cells,” *IEEE Transactions on Industrial Electronics*, vol. 61, pp. 2053–2061, 2014
- [2] H. Rahimi Eichi and M.-Y. Chow, “Modeling and analysis of battery hysteresis effects,” *2012 IEEE Energy Conversion Congress and Exposition (ECCE)*, pp. 4479–4486, 2012
- [3] H. Rahimi-Eichi, U. Ojha, F. Baronti, and M.-Y. Chow, “Battery management system: an overview of its application in the smart grid and electric vehicles,” *IEEE Industrial Electronics Magazine*, vol. 7, pp. 1–7, 2013.
- [4] F. Mocera and E. Vergori, “Battery performance analysis for working vehicle applications,” *IEEE Transactions on Industry Applications*, vol. 56, pp. 644–653, 2020.
- [5] Z. Wei, G. Dong, X. Zhang, J. Pou, Z. Quan, and H. He, “Noiseimmune model identification and state of charge estimation for lithium-ion battery using bilinear parameterization,” *IEEE Transactions on Industrial Electronics*, vol. 68, pp. 312–323, 2020.

- [6] Phillip Wiker, "A Systems 'Approach to Lithium-Ion Battery Management," ARTECH HOUSE, 2014
- [7] D. V. Do, C. Forgez, E. Kadri, K. Benkara, and G. Friedrich, "Impedance observer for a Li-ion battery using Kalman filter," IEEE Transactions on Vehicular Technology, vol. 58, pp. 3930–3937, 2009.
- [8] J. Xu, C. C. Mi, B. Cao, J. Deng, Z. Chen, and S. Li, "The state of charge estimation of lithium-ion batteries based on a proportional integral observer," IEEE Transactions on Vehicular Technology, vol. 63, pp. 1614–1621, 2014.
- [9] K. Sarrafan, K. M. Muttaqi, and D. Sutanto, "Real-time estimation of model parameters and state-of-charge of li-ion batteries in electric vehicles using a new mixed estimation model," IEEE Transactions on Industry Applications, vol. 56, pp. 5417–5428, 2020.
- [10] G. Fan, "Systematic parameter identification of a control-oriented electrochemical battery model and its application for state of charge estimation at various operating conditions," Journal of Power Sources, vol. 470, p.228153, 2020.
- [11] D. Zhang, S. Dey, H. E. Perez, and S. J. Moura, "Real-time capacity estimation of lithium-ion batteries utilizing thermal dynamics," IEEE Transactions on Control Systems Technology, vol. 28, pp. 992–1000, 2020.
- [12] Z. Wei, G. Dong, X. Zhang, J. Pou, Z. Quan, and H. He, "Noiseimmune model identification and state of charge

- estimation for lithium-ion battery using bilinear parameterization,” IEEE Transactions on Industrial Electronics, vol. 68, pp. 312–323, 2020.
- [13] B. Pattipati, C. Sankavaram, and K. Pattipati, "System Identification and Estimation Framework for Pivotal Automotive Battery Management System Characteristics", IEEE Transactions on Systems, Man, and Cybernetics, Part C (Applications and Reviews), vol. 41, no. 6, pp. 869-884, 2011.
- [14] Cheng Zhang; Kang Li; Sean Mcloone; Zhile Yang, “Battery Modelling Methods for Electric Vehicles - A Review”, IEEE Conference on European Control Conference (ECC: 24 July 2014),
- [15] Cheng Zhang; Kang Li; Sean Mcloone; Zhile Yang, “Battery Modelling Methods for Electric Vehicles - A Review”, IEEE Conference on European Control Conference (ECC: 24 July 2014),
- [16] M. Wang, A. Le, D. Noelle, Y. Shi, Y. Meng, and Y. Qiao, "Internal-short-mitigating current collector for lithium-ion battery", Journal of Power Sources, vol. 349, pp. 84-93, 2017.
- [17] B. Balagopal, C.-S. Huang, and M.-Y. Chow, “Effect of calendar aging on Li-ion battery degradation and SOH,” IECON 2017 - 43rd Annual Conference of the IEEE, pp. 7647–7652, 2017.
- [18] T. Huria, M. Ceraolo, J. Gazzarri and R. Jackey, "High fidelity electrical model with thermal dependence for characterization

- and simulation of high power lithium battery cells", IEEE International Electric Vehicle Conference, pp. 1-8, 2012.
- [19] H. Rahimi-Eichi, F. Baronti, and M. Y. Chow, " Modeling and online parameter identification of Li-Polymer battery cells for SOC estimation," in Proc. IEEE ISIE, 2012, pp. 1336–1341.
 - [20] Cong-Sheng Huang, and Mo-Yuen Chow, "Robust State-of-Charge Estimation for Lithium-ion Batteries over Full SOC Range" IEEE Journal. Industrial Electronics., Volu2, pp.305-313, July 2021.
 - [21] S. Abhinav and C. S. Manohar, "Bayesian parameter identification in dynamic state space models using modified measurement equations", Int. J. Non-Linear Mech., vol. 71, pp. 89-103, May 2015.
 - [22] Van der Merwe, Rudolph, and Eric A. Wan. "The Square-Root Unscented Kalman Filter for State and Parameter-Estimation." 2001 IEEE International Conference on Acoustics, Speech, and Signal Processing. Proceedings (Cat. No.01CH37221), 6:3461–64. Salt Lake City,UT,USA:IEEE,pp.61-64,2001.
 - [23] Simon, Dan. Optimal State Estimation: Kalman, H Infinity, and Nonlinear Approaches. Hoboken, NJ: John Wiley and Sons, 2006.
 - [24] H. Rahimi-Eichi and M.-Y. Chow, "Adaptive parameter identification and state-of-charge estimation of lithium-ion batteries," in Proc. 38th Annu. Conf. IEEE Ind. Electron. Soc., Montreal, QC, Canada, 2012, pp. 4012–4017.

- [25] A. J. Salkind, C. Fennie, P. Singh, T. Atwater, and D. E. Reisner, "Determination of state-of-charge and state-of-health of batteries by fuzzy logic methodology," *Journal of Power Sources*, vol. 80, no. 1-2, pp. 293–300, 1999.
- [26] P. Singh, R. Vinjamuri, X. Wang, and D. Reisner, "Design and implementation of a fuzzy logic-based state-of-charge meter for Li-ion batteries used in portable defibrillators," *Journal of Power Sources*, vol. 162, no. 2, pp. 829–836, 2006.
- [27] P. Singh, C. Fennie Jr., and D. Reisner, "Fuzzy logic modelling of state-of-charge and available capacity of nickel/metal hydride batteries," *Journal of Power Sources*, vol. 136, no. 2, pp. 322–333, 2004.
- [28] S. Malkhandi, "Fuzzy logic-based learning system and estimation of state-of-charge of lead-acid battery," *Engineering Applications of Artificial Intelligence*, vol. 19, no. 5, pp. 479–485, 2006.
- [29] Greg Welch and Gary Bishop, "An Introduction to the Kalman Filter," Department of Computer Science, University of North Carolina at Chapel Hill, Chapel Hill, North Carolina, USA, TR 95-041, 2006.
- [30] Ahmed Fasih, "Modeling and Fault Diagnosis of Automotive Lead-Acid Batteries," Columbus, Ohio, USA, April 2006.
- [31] V. Pop, H.J. Bergveld, D. Danilov, P.P.L. Regtien, and P.H.L. Notten, *Battery Management Systems.*: Springer, 2008.

- [32] I.-S. Kim, “Nonlinear state of charge estimator for hybrid electric vehicle battery,” *IEEE Trans. Power Electron.*, vol. 23, no. 4, pp. 2027–2034, Jul. 2008.
- [33] I.-S. Kim, “A technique for estimating the state of health of lithium batteries through a dual-sliding-mode observer,” *IEEE Trans. Power Electron.*, vol. 25, no. 4, pp. 1013–1022, Apr. 2010.
- [34] P. Shrivastava, T. K. Soon, M. Y. I. B. Idris, and S. Mekhilef, “Overview of model-based online state-of-charge estimation using Kalman filter family for lithium-ion batteries,” *Renewable and Sustainable Energy Reviews*, vol. 113, 2019.
- [35] Q. Yu, R. Xiong, R. Yang, and M. G. Pecht, “Online capacity estimation for lithium-ion batteries through joint estimation method,” *Applied Energy*, vol. 255, 2019.
- [36] C.-S. Huang and M.-Y. Chow, “Accurate Thevenin’s circuit-based battery model parameter identification,” 2016 IEEE 25th International Symposium on Industrial Electronics (ISIE), pp. 274–279, 2016.
- [37] C. Chen, R. Xiong, and W. Shen, “A lithium-ion battery-in-the-loop approach to test and validate multiscale dual H infinity filters for state-of-charge and capacity estimation,” *IEEE Transactions on Power Electronics*, vol. 33, pp. 332–342, 2018.
- [42] G. L. Plett, “Extended Kalman filtering for battery management systems of LiPB-based HEV battery packs—Part 2. Modeling

- and identification,” *J. Power Sources*, vol. 134, no. 2, pp. 262–276, Aug. 2004.
- [43] F. Zhang, G. Liu, L. Fang, and H. Wang, “Estimation of battery state of charge with H observer: Applied to a robot for inspecting power transmission lines,” *IEEE Trans. Ind. Electron.*, vol. 59, no. 2, pp. 1086–1095, Feb. 2012.
- [38] Y. Feng, C. Xue, Q. L. Han, F. Han, and J. Du, “Robust estimation for state-of-charge and state-of-health of lithium-ion batteries using integral type terminal sliding-mode observers,” *IEEE Transactions on Industrial Electronics*, vol. 67, pp. 4013–4023, 2020.
- [39] K. S. Ng, C.-S. Moo, Y.-P. Chen, and Y.-C. Hsieh, “Enhanced coulomb counting method for estimating state-of-charge and state-of-health of lithium-ion batteries,” *Appl. Energy*, vol. 86, no. 9, pp. 1506–1511, Sep. 2009.
- [40] F. Codeca, S. M. Savaresi, and V. Manzoni, “The mix estimation algorithm for battery state-of-charge estimator—Analysis of the sensitivity to measurement errors,” in *Proc. 48th IEEE CDC/CCC, Shanghai, China, Dec. 15–18, 2009*, pp. 8083–8088.
- [41] A. Zenati, P. Desprez, and H. Razik, “Estimation of the SOC and the SOH of Li-ion batteries, by combining impedance measurements with the fuzzy logic inference,” in *Proc. 36th*

Annu. Conf. IEEE IECON, Glendale, AZ, USA, Nov. 7–10, 2010, pp. 1773–1778.

- [42] G. L. Plett, “Extended Kalman filtering for battery management systems of LiPB-based HEV battery packs—Part 2. Modeling and identification,” *J. Power Sources*, vol. 134, no. 2, pp. 262–276, Aug. 2004.
- [43] F. Zhang, G. Liu, L. Fang, and H. Wang, “Estimation of battery state of charge with H observer: Applied to a robot for inspecting power transmission lines,” *IEEE Trans. Ind. Electron.*, vol. 59, no. 2, pp. 1086–1095, Feb. 2012.
- [44] F. Mocera and E. Vergori, "Battery performance analysis for working vehicle applications", *IEEE Trans. Ind. Appl.*, vol. 56, no. 1, pp. 644-653, 2020.
- [45] Xinfan Lin et al., "Parameterization and Observability Analysis of Scalable Battery Clusters for Onboard Thermal Management," in *Les Rencontres Scientifiques d'IFP Energies nouvelles – Int. Scient. Conf. on hybrid and electric vehicles*, December 2011.
- [46] Hector E Perez, Jason B Siegel, Xinfan Lin, and Yi Ding, "Parameterization and Validation of an Integrated Electro-Thermal Cylindrical LFP Battery Model," in *ASME Dynamic*

Systems Control Conference, Fort Lauderdale, Florida, USA, 2012.

- [47] W. B. Gu and C. Y. Wang, "Thermal-electrochemical modeling of battery systems," *Journal of The Electrochemical Society*, vol. 147, no. 8, pp. 2910–2922, 2000.
- [48] Q. Yu, R. Xiong, R. Yang and M. G. Pecht, "Online capacity estimation for lithium-ion batteries through joint estimation method", *Appl. Energy*, vol. 255, 2019.
- [49] C. Chen, R. Xiong and W. Shen, "A lithium-ion battery-in-the-loop approach to test and validate multiscale dual h. infinity filters for state-of-charge and capacity estimation", *IEEE Trans. Power Electron.*, vol. 33, no. 1, pp. 332-342, 2018
- [50] C. Zhang, K. Li, L. Pei and C. Zhu, "An integrated approach for real-time model-based state-of-charge estimation of lithium-ion batteries", *J. Power Sour.*, vol. 283, pp. 24-36, 2015.
- [51] G. Fan, "Systematic parameter identification of a control-oriented electrochemical battery model and its application for state of charge estimation at various operating conditions", *J. Power Sour.*, vol. 470, 2020.

- [52] F. Mocera and E. Vergori, "Battery performance analysis for working vehicle applications", *IEEE Trans. Ind. Appl.*, vol. 56, no. 1, pp. 644-653, 2020.